

Using Graviton EFT and Massive Gravity to Compute Gravitational Potentials for Black Hole Inspirals

Thesis by
Bethany Anne Suter

In Partial Fulfillment of the Requirements for the
Degree of
Bachelor of Science

The logo for the California Institute of Technology (Caltech), featuring the word "Caltech" in a bold, orange, sans-serif font.

CALIFORNIA INSTITUTE OF TECHNOLOGY
Pasadena, California

2020
Defended June 4, 2020

© 2020

Bethany Anne Suter
ORCID: 0000-0002-4503-5771

All rights reserved

ACKNOWLEDGEMENTS

I would like to thank the SURF program and the SFP office for their support and encouragement throughout the summer. I would also like to thank Professor Clifford Cheung for taking me on as a mentee and facilitating my research throughout the summer and rest of the year. In addition, I truly appreciate the time that Mikhail Solon took out of his busy schedule to answer my abundant questions. Finally, I would like to express my extreme gratitude to Mr. and Mrs. Haaga for funding my SURF this summer. Without all of your support and kindness, this summer would not have been nearly as successful or enjoyable.

ABSTRACT

This year, the LIGO detectors entered their third observing run and have been detecting black hole interactions with increasing precision and sensitivity. These detections have opened up a new way to compare the predictions of Einsteinian gravity with more exotic models. One of these models, massive gravity, is a concrete toy to use in testing these predictions. This project uses ideas from EFT and standard techniques from quantum field theory to calculate scattering amplitudes for scalar particles interacting via gravitons. We first calculated amplitudes up to the 1-loop level assuming the standard massless graviton and then assuming a massive graviton. We then mapped these amplitudes to gravitational potentials for black holes. Future work will include looking at the different predictions of these two theories (massless and massive gravitons), and comparing them to black hole inspiral data to determine if the massive graviton theory could be a legitimate contender as a model for gravity.

TABLE OF CONTENTS

Acknowledgements	iii
Abstract	iv
Table of Contents	v
List of Illustrations	vii
Chapter I: Introduction	1
Chapter II: Effective Field Theory	3
2.1 Background	3
2.2 Graviton EFT	4
2.3 From Scattering Amplitudes to Black Hole Inspirals	7
2.4 A Higher Order Calculation	8
Chapter III: Massive Gravity	10
3.1 Introduction	10
3.2 Motivations for a Massive Graviton	10
3.3 History	11
Chapter IV: Feynman Diagrams	16
4.1 The Basic Feynman Rules	16
4.2 Changes in the Feynman Rules due to Massive Gravity	17
4.3 The Nonanalytic Component of the Scattering Matrix	18
Chapter V: Tree Level Amplitudes	20
5.1 Massless Graviton Interactions	20
5.2 Massive Graviton Interactions	21
Chapter VI: One-loop Modification (Massless)	23
6.1 Techniques	23
6.2 Results	24
6.3 Analysis of Full Potential	30
Chapter VII: Integration with a Massive Graviton	32
7.1 Scalar Integrals	33
7.2 Passarino-Veltman Decomposition	33
7.3 Tensor Integrals	36
Chapter VIII: One-loop Modification (Massive)	37
8.1 Classical vs Quantum	37
8.2 Techniques	37
8.3 Results for Classical Diagrams	37
8.4 Classical Discussion	41
8.5 Results for Quantum Diagrams	42
Chapter IX: Future Work	47
Bibliography	48
Appendix A: Vertices and Propagators	51
A.1 Massive Scalar Propogator	51

A.2 Massless Graviton Propogator	51
A.3 Massive Graviton Propagator	51
A.4 Massless Ghost Propagator	51
A.5 2 Scalar, 1 Graviton Vertex Factor	52
A.6 2 Scalar, 2 Graviton Vertex Factor	52
A.7 3 Graviton Vertex Factor	53
A.8 2 Ghost, 1 Graviton Vertex Factor	53
Appendix B: Integrals used in the Massless Case	54
B.1 Bubble Integrals	54
B.2 Triangle Integrals	54
B.3 Box and Cross Box Integrals	55
Appendix C: Integrals used in the Massive Case	56
C.1 Tadpole and Bubble Integrals	56
C.2 Triangle Integrals	59
C.3 Box and Cross Box Integrals	63
Appendix D: Fourier Transforms	64
Appendix E: Color-Kinematics Duality	65

LIST OF ILLUSTRATIONS

<i>Number</i>	<i>Page</i>
2.1 A simple scalar-graviton interaction	6
2.2 A summary of known results for the two-body potential for spinless black holes in the PN and PM expansions, outlined in blue and green regions respectively. We are calculating at 2PM, directly above the red highlighted section. Figure taken from [2].	9
4.1 A generic Feynman diagram, with external lines labeled (internal lines not shown). Figure and caption taken from [32]	16
5.1 The Tree Level Diagram. Figure taken from [5]	20
6.1 The box and crossed box diagrams which contribute to the nonanalytic component of the potential. Figure and caption taken from [5].	24
6.2 The set of triangle diagrams contributing to the scattering amplitude. Figure and caption taken from [5].	26
6.3 The double-seagull contribution to the scattering amplitude. Figure and caption taken from [5].	27
6.4 The class of the graviton vertex correction diagrams which yield nonanalytic corrections to the potential. Figure and caption taken from [5].	28
6.5 The vacuum polarization diagrams which contribute to the potential. Note that there exists a ghost diagram along with the graviton loop. Figure and caption taken from [5].	29
E.1 A tree level gluon interaction	65
E.2 A tree level graviton interaction	66

Chapter 1

INTRODUCTION

Although many physicists have attempted to make major breakthroughs in the field of quantum gravity, as of now, it is challenging to reconcile the fields of gravity and quantum mechanics at all energies. However, the ideas of effective field theory (EFT) have taken root in many theorists' consciousnesses and are birthing a new method of examining how gravity and quantum field theory may still be able to work together. These ideas provide a realistic means of calculating scattering amplitudes for sources coupled by gravitons. In particular, new research in EFT is now being done to allow us to calculate the scattering amplitudes of black holes. These scattering amplitudes can actually be simply mapped to gravitational potentials for binary black hole systems at higher orders than is usually possible through existing perturbative methods from general relativity. These new and more accurate potentials can be used by the Laser Interferometer Gravitational-Wave Observatory or LIGO to calculate the inspirals and mergers for these black holes. As LIGO is currently in its third observing run and is detecting more events than ever, this research into creating more accurate models for fitting LIGO waveforms is more important than ever. In addition, this ease of calculation of gravitational potentials through effective field theoretic means has opened the opportunity to test theories beyond Einsteinian gravity. In particular, it is possible to calculate gravitational amplitudes and thus potentials for these new theories and compare them to the predictions of general relativity. By comparing both predictions to LIGO's observations, it is possible to determine which of the theories is a better fit to what we see.

In this project, we look at one specific theory beyond general relativity, massive gravity. We examine how the addition of a graviton mass may change the gravitational potentials of black hole binaries. We use the techniques of quantum field theory and effective field theory to quantize general relativity in the low energy regimes and calculate the scattering amplitudes for the interaction of two massive scalar particles mediated by massive gravitons. After mapping the amplitudes to gravitational potentials, we compare the predictions of this more exotic theory of gravity to those of the regular Einsteinian model which assumes a massless graviton.

In the second chapter, we begin by describing the methods of effective field theory

and how it can be used to quantize general relativity. We also illustrate the path from scattering amplitudes to potentials of black holes and describe the benefits of this particular method. Chapter 3 outlines the history and motivations for pursuing the theory of massive gravity. In Chapter 4, we describe the purpose of Feynman diagrams and Feynman rules as well as how the basic rules change with respect to massive gravity. The fifth chapter uses the methods of effective field theory to find the Newtonian potential from the tree level amplitudes for the case of the massless graviton. We then derive how the amplitude shifts to produce a Yukawa potential when a graviton mass is included. In Chapter 6, we rederive previous calculations at the one-loop level for the massless graviton. We follow the work of Bjerrum-Bohr et. al. and Holstein, and find consistent results [5, 20]. Chapter 7 describes the changes in integration due to the graviton mass as well as the process of finding these new integrals. In Chapter 8, we move on to the one-loop level for the massive graviton. We relate our results for both the classical and quantum diagrams and discuss their relation to the corresponding results in the massless graviton case. Finally, in Chapter 9, we look at various ways to add to this project, confirm our results, and formulate future projects.

Chapter 2

EFFECTIVE FIELD THEORY

2.1 Background

The history of physics is a history of approximations, a history of theories that work in a specific regime but fail dramatically when extended out of those regimes. Yet it is that moment of failure which opens up new realms of ideas and new physics. Classical mechanics, while incredibly accurate in everyday life, gives way to quantum mechanics when looking at the very smallest parts of our universe. Newtonian gravity, enough to explain Earth's orbit around the sun, fails to comprehend the ideas of black holes or gravitational lensing which are born from the tenets of general relativity. Even in particle physics, this idea of different theories working at successive energy scales is not foreign. While we normally treat the electromagnetic, weak, and strong forces as separate forces and theories, the Standard Model says that at high enough energies, their relative strengths are approximately equal, suggesting an underlying symmetry connecting all of them and forming a theory described by a singular Lagrangian.

Because of this wide acceptance of theories that only work in specific realms, the ideas of effective field theory should follow naturally. EFT is a way of thought that does not require theories to be accurate at high energies, but instead looks at their predictive power in the low energy regime [11]. EFT accepts that certain theories might not be full descriptions of reality since they fail when taken to the highest energy limits, but realizes that they could still reveal new knowledge about the universe in the realms where they do apply. In particle physics, this means that theories that were once rejected due to nonrenormalizability can now be used and gleaned for useful truths.

More practically, how does EFT accomplish these lofty goals? In regular quantum mechanics, physicists use perturbation theory when they do not have full information about higher energy states. They are able to do this because these higher energy states usually contribute much less to the interactions since they are harder to access. EFT attempts to do a similar thing for quantum field theory. Due to the Heisenberg Uncertainty Principle, physicists know that the higher the energy of an interaction, the shorter distance it will be able to cover. This means that the super

high energy contributions to interactions in quantum field theory will only contribute to very local interactions. If we are interested in long-distance interactions, these higher energy (singular) interactions can be neglected. Thus, another definition of EFT, as said by Donoghue [12], is that "effective field theory is then the procedure for describing the long-distance physics [...] that are active at low energy." This procedure can be used both for theories where the entire theory is known or for those where it is only partially known; in both we are then able to use an effective Lagrangian to describe the theory.

2.2 Graviton EFT

While EFT is a very general theory for describing phenomena in lower energy regimes, it has found its greatest success in the realm of quantum gravity. For a long time, the theories of general relativity and quantum mechanics were considered to be incompatible. This is due to the fact that the quantized version of general relativity is what is known as a nonrenormalizable theory. When extended to extremely high energies on the order of the Planck mass, the theory fails and produces an infinite set of infinities. While they can be renormalized away, due to their infinite number, the theory loses any predictive power. However, general relativity is actually one of the most accurate theories physicists have today, only needing a few quantum corrections up to the Planck scale. It is this combination of characteristics that make general relativity a perfect candidate for the methods of EFT [11].

Review of General Relativity

Before we can quantize general relativity, it is important to define all the many terms and conventions we will be using. Throughout the rest of this thesis, we will be using the convention that $\hbar = c = 1$ as well as the minus metric convention (+1, -1, -1, -1).

We have defined the Christoffel symbols or connection coefficients to be the usual expression:

$$\Gamma^{\lambda}_{\alpha\beta} = \frac{g^{\lambda\sigma}}{2} [\partial_{\alpha}g_{\beta\sigma} + \partial_{\beta}g_{\alpha\sigma} - \partial_{\sigma}g_{\alpha\beta}] \quad (2.1)$$

which all have one derivative of the metric.

Similarly, we have that the curvatures (Riemann tensor, Ricci tensor, and Ricci

scalar , respectively) are:

$$R^\mu{}_{\nu\alpha\beta} \equiv \partial_\alpha \Gamma^\mu{}_{\nu\beta} - \partial_\beta \Gamma^\mu{}_{\nu\alpha} + \Gamma^\mu{}_{\sigma\alpha} \Gamma^\sigma{}_{\nu\beta} - \Gamma^\mu{}_{\sigma\beta} \Gamma^\sigma{}_{\nu\alpha} \quad (2.2)$$

$$R_{\mu\nu} = R^\alpha{}_{\mu\alpha\nu} = \partial_\alpha \Gamma^\alpha{}_{\mu\nu} - \partial_\nu \Gamma^\alpha{}_{\mu\alpha} + \Gamma^\alpha{}_{\sigma\alpha} \Gamma^\sigma{}_{\mu\nu} - \Gamma^\alpha{}_{\sigma\nu} \Gamma^\sigma{}_{\mu\alpha} \quad (2.3)$$

$$R = g^{\mu\nu} R_{\mu\nu} = g^{\mu\nu} \partial_\alpha \Gamma^\alpha{}_{\mu\nu} - g^{\mu\nu} \partial_\nu \Gamma^\alpha{}_{\mu\alpha} + g^{\mu\nu} \Gamma^\alpha{}_{\sigma\alpha} \Gamma^\sigma{}_{\mu\nu} - g^{\mu\nu} \Gamma^\alpha{}_{\sigma\nu} \Gamma^\sigma{}_{\mu\alpha} \quad (2.4)$$

which each have two derivatives of the metric.

From classical general relativity, we get a Lagrangian that takes the simple form:

$$\mathcal{L} = \sqrt{-g} \left[\frac{2R}{\kappa^2} + \mathcal{L}_{matter} \right] \quad (2.5)$$

where $\kappa^2 = 32\pi G$, g is the determinant of the metric $g_{\mu\nu}$ and \mathcal{L}_{matter} is the covariant Lagrangian for the matter fields in the theory (scalars, fermions, etc.), and R is again the Ricci Scalar.

Quantifying GR via EFT

For Eq. 2.5 to describe an effective field theory, we must account for other higher derivative couplings of the fields using the curvatures. Since the Lagrangian must be a scalar, we can see that the extra terms can take the following form in order of increasing derivatives:

$$\mathcal{L}_{EFT} = \sqrt{-g} \left[\frac{2R}{\kappa^2} + c_1 R^2 + c_2 R_{\mu\nu} R^{\mu\nu} + \dots + \mathcal{L}_{matter} \right] \quad (2.6)$$

The ellipses take into account all possible higher derivative terms that must be included. There can also be higher derivative terms that must be added to the matter Lagrangian due to this being an effective field theory. The coupling factors are determined via empirical calculation, but the only current constraints on them are that c_1 and c_2 must be both smaller than 10^{+74} as found by the experiment in [33]. However, the natural expectation is that these gravitational couplings are generated by Planck scale quanta, which would set $c_1, c_2 \sim 1$. In addition, we do know that the curvature squared terms are expected to be incredibly tiny on regular energy scales. While these terms could possibly cause instabilities at energies above the Planck scale, EFT only holds below this scale anyway, so there are no contradictions and this is not an issue with the theory.

The Graviton

The quantized version of general relativity requires a different interpretation of gravity than one is used to. General relativity claims that gravity is fully geometric,

that the apparent force of gravity is in fact due to curvature in space-time created by matter in that space-time. Since curved space-time requires one to use differential geometry and other complicated mathematics, often physicists will examine regions of space-time far from any matter. In these low-gravity regions, it is possible to find a linearized perturbation off of flat space-time as seen below.

$$g^{\mu\nu} = \eta^{\mu\nu} + h^{\mu\nu} \quad (2.7)$$

where η is the flat space metric and h is the small perturbation tensor. In this approximation, h acts almost like a field since it has values at every point in space and time. If one finds the equation of motion of this tensor, it is actually the origin of the prediction of gravitational waves. These small bits of curvature propagate out from massive objects at the speed of light and exert the force of gravity on the surrounding space and matter.

However, when general relativity is quantized, this picture changes. Since we are now in the realm of particle physics and quantum field theory, the gravitational force is now said to be mediated by a spin 2 boson called the graviton. Since it is spin 2, its field is actually represented by a rank 2 tensor which perfectly correlates to the $h^{\mu\nu}$ seen in general relativity, only now it is interpreted as a field instead of curvature. The graviton is massless, so it is still expected to propagate at the speed of light, just like the gravitational waves from above. This theoretical particle has not yet been observed empirically, but doing so would confirm the success of EFT's interpretation of gravity.

The Simplest Model of Interaction

Above we said that in this theory, the graviton now mediates the gravitational force. But how does this actually occur? This process and the ensuing calculation will change depending on what type of particles are interacting via gravity. However, for simplicity's sake, this thesis will only look at how scalar particles interact via gravitons. In fig 2.1, we see the most simple interaction - one massive scalar particle emitting a graviton and the other particle absorbing it. The solid lines represent the scalar particles, while the double squiggle is the path of the graviton. p_i represents the momenta of the incoming and outgoing particles, while

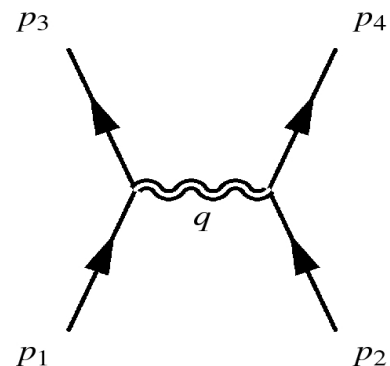


Figure 2.1: A simple scalar-graviton interaction

q is the momenta exchanged between the two scalar particles. This diagram is a Feynman diagram and is built to describe particle interactions as well as provide a means to find the probability of those interactions occurring. This calculation is known as a scattering amplitude, since these particles are considered to be scattering off of one another.

The Gravitational Potential

These scattering amplitudes and diagrams are useful because they allow us to find the gravitational potentials of these two scalar particles. However, this mapping is not immediately obvious and there is not one conventional method; many different papers have used various means of finding these potentials [9, 23, 26, 29]. We have chosen to use the same method as used by Bjerrum-Bohr et. al. [5] - simply mapping the full scattering amplitude to the potential itself via the Born approximation. They defined the potential via the following formula:

$$\begin{aligned}\langle f|T|i\rangle &\equiv (2\pi)^4 \delta^{(4)}(p - p') \mathcal{M}(q) \\ &= -(2\pi) \delta(E - E') \langle f|\tilde{V}(q)|i\rangle\end{aligned}\quad (2.8)$$

where p and p' are the incoming and outgoing four-momenta. We can convert this into a calculation of the coordinate-space potential by taking the non-relativistic limit and Fourier-transforming. While the normal non-relativistic normalization equation takes the form $\frac{1}{(2E_1)(2E_2)}$, we drop the velocity corrections, producing the formula $\frac{1}{(2m_1)(2m_2)}$, resulting in:

$$\frac{1}{2m_1} \frac{1}{2m_2} \int \frac{d^3q}{(2\pi)^3} e^{i\mathbf{q}\cdot\mathbf{x}} \mathcal{M}(\vec{q}) \quad (2.9)$$

It must be noted that there are other methods to calculate the potential from the scattering amplitude. In particular, we could subtract off the second order contributions from the Born approximation. We chose the first method since we are only looking at leading order behavior and this more complex method would simply increase the amount of work for no extra benefit at this order. This potential $\tilde{V}_{bs}(q)$ is used in bound state quantum mechanics and can be simply related to our defined potential at this order via:

$$V_{bs}(r) = V(r) + \frac{7Gm_1m_2(m_1 + m_2)}{2c^2r^2} \quad (2.10)$$

2.3 From Scattering Amplitudes to Black Hole Inspirals

We have now been able to make the transition from scattering amplitudes to gravitational potentials. However, we are still solidly in the realm of particle physics.

How can we connect this back to the idea of black holes? Well, those massive scalar particles from the above section have very few constraints. They must simply be massive, scalar and particle like. However, we know of another object that is extremely massive: the black hole. Additionally, while most observed black holes have a net angular momentum, and are thus not scalar, we can consider the most basic spinless black hole. Our calculation will also still apply to other black holes at zeroth order in spin, i.e. ignoring spin completely. While spin is important, we consider the simplest case here. Finally, we also assume that the distance between the two black holes is much much larger than their finite size. For black holes, these finite size effects enter at 5PM, i.e. 5-loops relative to this 1-loop calculation (see Section 2.4 for full explanation of PM order counting). This effect is known as the "effacement theorem." Thus, for the sake of our 1-loop calculation, we can also treat black holes as point-like particles. Putting this all together, we can see that we can simply map these particle interactions to interactions between black holes. Using this mapping, those gravitational potentials that we calculated are now the gravitational potentials of two black holes. With these potentials, one can create models for black hole binary inspirals - just like those LIGO uses to make detections.

2.4 A Higher Order Calculation

This new method is incredibly important because it actually finds these potentials at higher order than is usually feasible via numerical relativity. Normal numerical relativistic calculations keep track of post-Newtonian (PN) orders using two small factors:

$$v^2 \sim \frac{GM}{|r|} \ll 1 \quad (2.11)$$

where M is the total mass of the binary system, and r and v are the relative position and velocity of the two black holes. The virial theorem tells us that these two quantities (corresponding to the kinetic and potential energies) should be approximately the same magnitude. The PN expansion is a double expansion with respect to both of these small quantities. However, this new procedure using EFT introduces a new type of expansion, called the post-Minkowskian expansion (PM) [2]. As seen in fig. 2.2, this new expansion actually calculates all orders in v^2 at the same time and then calculates order by order in G . The PM expansion produces far more information at lower orders in the calculation, but can also be used simultaneously with the regular PN expansion as shown by the green rectangles. Due to this convenient mechanism, this method of calculation requires much less computing power and complex mathematics than numerical relativistic calculations

	0PN	1PN	2PN	3PN	4PN	5PN	6PN	7PN		
1PM	(1	+ v ²	+ v ⁴	+ v ⁶	+ v ⁸	+ v ¹⁰	+ v ¹²	+ v ¹⁴	+ ...)	G ¹
2PM		(1	+ v ²	+ v ⁴	+ v ⁶	+ v ⁸	+ v ¹⁰	+ v ¹²	+ ...)	G ²
3PM			(1	+ v ²	+ v ⁴	+ v ⁶	+ v ⁸	+ v ¹⁰	+ ...)	G ³
4PM				(1	+ v ²	+ v ⁴	+ v ⁶	+ v ⁸	+ ...)	G ⁴
5PM					(1	+ v ²	+ v ⁴	+ v ⁶	+ ...)	G ⁵
6PM						(1	+ v ²	+ v ⁴	+ ...)	G ⁶
										⋮

Figure 2.2: A summary of known results for the two-body potential for spinless black holes in the PN and PM expansions, outlined in blue and green regions respectively. We are calculating at 2PM, directly above the red highlighted section. Figure taken from [2].

do. This method has been used by Cheung et. al. to do these scattering amplitude calculations up to the two loop level, which has immense applications for LIGO [2]. These new and more accurate potentials can be used by LIGO to calculate the inspirals of black hole binary systems. Since LIGO's third observing run is currently running, this research into creating more accurate models that will be used to fit waveforms is more important than ever before.

However, this method has other applications besides just aiding LIGO's search for more merger events. It also creates an opportunity to test the predictions of more exotic theories of gravity. EFT's method approaches a problem normally solidly in the realm of general relativity and shapes it into a particle theory problem. This opens up the theory to take from a far wider range of challengers to traditional Einsteinian gravity and determine how their predictions weigh against those of quantized general relativity. In particular, one of these theories, massive gravity, shows promise and will be discussed throughout the rest of this thesis.

Chapter 3

MASSIVE GRAVITY

3.1 Introduction

In the most straightforward way, massive gravity is a modification to general relativity that is formed when we simply add a mass term to the Einstein-Hilbert Lagrangian which would give the graviton a mass m . We should expect that as $m \rightarrow 0$, the theory should return to classical general relativity and retrieve those results. At this point, several different studies have tried to constrain this graviton mass. In particular, a study looking at its effect on weak gravitational lensing established that $m < 6 \times 10^{-32}$ eV, while another study examining gravitational waves from LIGO constrained the mass to be less than 6.76×10^{-23} eV [3, 8]. While these are different in magnitude, it still gives an idea for how small this mass would need to be to match experimental results.

One important consequence of changing from a massless graviton theory to a massive graviton theory is the addition of 3 extra degrees of freedom. While a massless spin two particle has two helicity states, the massive graviton has five polarizations, along both the transverse and longitudinal axes. As a warning, these extra degrees of freedom cause many of the issues with the theory of massive gravity, so this will come up again and again in this chapter.

3.2 Motivations for a Massive Graviton**Testing Einstein**

Although general relativity is one of the most accurate theories that physicist know of today, it still has some major issues. In particular, when one tries to extend the quantized version of the theory beyond the Planck scale, the theory completely breaks down. This means that general relativity simply cannot be the full description of gravity. This issue provides a great incentive to create theories that would fix these problems. However, that is impossible without testing the theory thoroughly. One common method of testing a theory involving a massless particle is by giving that particle a small but non-negligible mass and seeing how the dynamics of the system shift perturbatively. This process not only determines if the particle might be better described by slightly massive particle, but also provides a method of exploring the limits of the original theory. Massive gravity exactly fits this narrative. One

of the major goals of the theory of massive gravity is to see if this description of gravity provide a cohesive picture that could even be extended to energies greater than the Planck scale.

The Cosmological Constant Problem

One of the most pressing issues in cosmology today is explaining the small but nonzero value of the cosmological constant. While current theories usually insert the hypothesis of dark energy, some unknown energy with negative pressure, there is a lot of skepticism for this explanation. However, massive gravity is able to provide an natural explanation for the small value of the cosmological constant. At first order, the force mediated by a massive graviton takes the form $\sim \frac{1}{r}e^{-mr}$. As r is increased, the field will diminish exponentially from that of the massless graviton. If we set the graviton mass to be on the order of the Hubble constant ($m \sim H$), then we should see the effect of gravity fall off just as the Hubble expansion predicts. This provides a natural explanation for the small cosmological constant since it is now explained by the mass of a particle. In addition, Vainshtein screening, as discussed in 3.3, provides some rationale for why we do not see this exponential decay on the scale of a galaxy, but only in cosmological distances. While there are still some issues with this specific explanation of the cosmological constant, massive gravity as a whole shows promise, in particular in fields such as bigravity[1, 18].

3.3 History

Fiers-Pauli Theory

In the 1930s, the first theory of massive gravitons was developed by Pauli and Fierz [19]. They wrote down the action for a single massive spin 2 particle in Minkowski space with the field defined to be a symmetric rank two tensor $h_{\mu\nu}$. This action, usually known as the *Fierz-Pauli action* is shown below [19]:

$$S = \int d^Dx \left[-\frac{1}{2}\partial_\lambda h_{\mu\nu}\partial^\lambda h^{\mu\nu} + \partial_\mu h_{\nu\lambda}\partial^\nu h^{\mu\lambda} - \partial_\mu h^{\mu\nu}\partial_\nu h + \frac{1}{2}\partial_\lambda h\partial^\lambda h - \frac{1}{2}m^2(h_{\mu\nu}h^{\mu\nu} - h^2) \right] \quad (3.1)$$

To partially rationalize this choice of action, we note that this choice contains all possible contractions of h with two or fewer derivatives. Importantly, it also includes the desired mass term. Once that mass m is taken to zero, this action matches the linearized form of the Einstein-Hilbert action.

One other thing to note about this action is the Fiers-Pauli tuning, the name for the relative factor of -1 chosen to be between the two mass terms. If we violate the tuning,

and introduce a nonzero, dimensionless a , forming $-\frac{1}{2}m^2(h_{\mu\nu}h^{\mu\nu} - (1-a)h^2)$, we actually get an action has an extra (sixth) degree of freedom. This extra degree of freedom in the Lagrangian describes a scalar ghost with negative kinetic energy of mass $m_g^2 = \frac{3-4a}{2a}m^2$. For small a , this ghost's mass goes as $\sim \frac{1}{a}$, which clearly goes to infinity in the limit $a \rightarrow 0$ or equivalently, when we try to return to the Fiers-Pauli tuning. This infinite mass renders the ghost particle non-dynamical and unphysical. However, using the tuning from the beginning carefully eliminates the issue, by removing that extra degree of freedom and thereby the ghost field.

The vDVZ Discontinuity

In its most essential elements, the vDVZ discontinuity describes the result of taking the theory of massive gravity and returning to the more traditional theory by taking the limit as the graviton mass vanishes. Unfortunately, as clued in by the name, there is a discontinuity there. The easiest method to find this discontinuity is through looking at how light would be expected to bend around a heavy object. In regular, linearized general relativity, we can examine how a test particle might be effected by a small perturbation of curvature $h_{\mu\nu}$. Referring to textbooks, we find that if we constrain the field $h_{\mu\nu}$ to take the form $\frac{2h_{00}}{M_P} = -2\phi$, $\frac{2h_{ij}}{M_P} = -2\psi\delta_{ij}$, and $h_{0i} = 0$ for some functions $\phi(r)$ and $\psi(r)$, and where M_P is the Planck mass, then we know that the Newtonian potential felt by the particle should simply be $\phi(r)$. If we define $\psi(r) = \gamma\phi(r)$ and $\phi(r) = -\frac{k}{r}$ for some constants γ and k , then the angle for the bending of light with impact parameter b must be

$$\alpha = \frac{2k(1+\gamma)}{b}. \quad (3.2)$$

Matching this structure with the massless graviton case, we know that

$$\phi(r) = \psi(r) = -\frac{GM}{r}, \quad \text{massless graviton} \quad (3.3)$$

and thus $\gamma = 1$ and $k = GM$. The bending angle becomes:

$$\alpha = \frac{4GM}{b}, \quad \text{massless graviton} \quad (3.4)$$

In the massive graviton case, as will be shown later, the metric is not in the right form to plug into the above equations. However, since we have assumed the coupling to the test particle to be gauge invariant, we are free to do a gauge transformation on

our solution for $h_{\mu\nu}$, producing:

$$h_{00} = \frac{2M}{3M_P} \frac{1}{4\pi} \frac{e^{-mr}}{r}, \quad (3.5)$$

$$h_{0i} = 0, \quad (3.6)$$

$$h_{ij} = \frac{M}{3M_P} \frac{1}{4\pi} \frac{e^{-mr}}{r} \delta_{ij} \quad (3.7)$$

Taking the limit $m \rightarrow 0$, we get that the potential terms are:

$$\phi(r) = -\frac{4}{3} \frac{GM}{r}, \psi(r) = -\frac{2}{3} \frac{GM}{r}, \quad \text{massive graviton} \quad (3.8)$$

In this case, we now have $\gamma = \frac{1}{2}$ and $k = \frac{4GM}{3}$. Plugging this back into eq. 3.2, we get

$$\alpha = \frac{2(\frac{4GM}{3})(1 + \frac{1}{2})}{b} = \frac{4GM}{b}, \quad \text{massive graviton} \quad (3.9)$$

However, if we wish to rescale G , so that our potential matches the Newtonian potential ($G \rightarrow \frac{3}{4}$), then the bending angle would change to

$$\alpha = \frac{3GM}{b}, \quad \text{massive graviton} \quad (3.10)$$

which is off by 25% from GR's prediction. This vDVZ discontinuity violates ones intuition that the parameters of nature should be able to transition smoothly to zero - there should not be a way to tell if a parameter is nonzero simply by a finite measurement.

The Stückelberg Trick

While this puzzling discontinuity stuck for quite a while, and stalled research in the field of massive gravity, eventually some contemporary physicists realized that they could apply work done previously by Stückelberg for a different application. Their realization was that the issue with trying to take the limit $m \rightarrow 0$ was due to the extra degrees of freedom necessitated by the massive graviton. The gauge symmetry that eliminates those three degrees of freedom only appears when the mass is zero. Taking the limit from the massive graviton to the massless graviton attempts to remove those degrees of freedom without providing a way for them to vanish. However, Stückelberg realized that if one introduced both a massless vector and a massless scalar (with 2 and 1 degrees of freedom, respectively) into the massive theory without changing it (via gauge symmetries), these new particles would decouple in the limit $m \rightarrow 0$. When these extra particles are included, the extra degrees of freedom are no longer lost and the limit is once again smooth.

This process of introducing extra massless fields to accommodate extra degrees of freedom is called the Stückelberg trick, after the original physicist who discovered this method. However, the expense of removing the vDVZ discontinuity is high - any calculation attempting to do so would need to include all possible interactions due to these extra fields.

Vainshtein Screening

Another potential solution to the vDVZ discontinuity is that of Vainshtein screening. Vainshtein investigated how including nonlinearities into the theory would effect the results. He found that around any massive object, such as a star of mass M , there is a new length scale associated with it known as the Vainshtein radius, $r_V \sim \left(\frac{M}{m^4 M_p^2}\right)^{1/5}$. At distances less than this length scale, non-linearities actually dominate the theory and any predictions of the linear theory cannot be trusted. Indeed, if we take the limit as $m \rightarrow 0$, the Vainshtein radius goes to infinity and none of the linear results can be trusted in any realm. This actually opens up the opportunity for these non-linear effects to remove the vDVZ discontinuity. To introduce some numbers into this calculation, let us assume M is one solar mass and m is approximately the Hubble constant $m \sim 10^{-33} eV$. This gives us an $r_V \sim 10^{18}$ or approximately the size of the Milky Way [19]. These changes also lead to one of the motivations for massive gravity as a theory which we discussed in section 3.2.

The Boulware-Deser Ghost

However, this idea of Vainshtein screening introduced new issues of its own. Boulware and Deser examined some of the fully nonlinear theories and determined that they contained an extra (sixth) degree of freedom with negative kinetic energy [6]. This became aptly known as the Boulware-Deser ghost. This ghost occurs because the Fierz-Pauli tuning, which worked so well for linear massive gravity, is no longer able to fully cancel out this extra mode when the nonlinear terms are included. For many years, this ghost was thought to be unavoidable - that all versions of massive gravity would contain it. This idea again stalled out the field until 2010.

dRGT Massive Gravity

In 2010, de Rham, Gabadadze, and Tolley discovered a massive gravity theory with nonlinear terms that had the coefficients precisely tuned to eliminate the Boulware-Deser ghost. The action for the ghost-free dRGT (de Rham-Gabadadze-Tolley)

massive gravity is given by [17] as:

$$S = \int d^4x \sqrt{-g} \left(-\frac{M_P l^2}{2} R + m^2 M_P^2 \sum_{n=0}^4 \beta_n e_n(\mathbb{X}) + \mathcal{L}_{matter} \right) \quad (3.11)$$

Similarly to in Fierz-Pauli's original theory, the first term (proportional to the Ricci scalar R) is still identical to the Einstein-Hilbert action and there is again a minimal coupling to the matter Lagrangian. However, the middle term is new and is a carefully constructed and tuned mass term.

We will here define all the various terms used in this term. First, we define $\mathbb{X} = \sqrt{g^{-1}f}$ or equivalently in index notation, $X^\mu_\alpha X^\alpha_\nu = g^{\mu\alpha} f_{\nu\alpha}$ where $g_{\mu\nu}$ is the normal metric and $f_{\mu\nu}$ is a reference metric which corresponds to the background metric around which the Pauli-Fierz fluctuations take place. Thus, for most calculation's purposes, we can take $f_{\mu\nu} = \eta_{\mu\nu}$, although this formulation is generalized for any background metric. The β_i are dimensionless coupling constants which are usually considered to be $O(1)$. We can also define the elementary symmetric polynomials e_n as:

$$e_0(\mathbb{X}) = 1, \quad (3.12)$$

$$e_1(\mathbb{X}) = [\mathbb{X}] \quad (3.13)$$

$$e_2(\mathbb{X}) = \frac{1}{2}([\mathbb{X}]^2 - [\mathbb{X}^2]) \quad (3.14)$$

$$e_3(\mathbb{X}) = \frac{1}{6}([\mathbb{X}]^3 - 3[\mathbb{X}][\mathbb{X}^2] + 2[\mathbb{X}^3]) \quad (3.15)$$

$$e_4(\mathbb{X}) = \det \mathbb{X} \quad (3.16)$$

where $[\mathbb{X}]$ indicates the trace of \mathbb{X} or X^μ_μ . This particular antisymmetric combination of terms in each e_n fully eliminates the Boulware-Deser ghost from the calculation.

FEYNMAN DIAGRAMS

4.1 The Basic Feynman Rules

In quantum field theory, one of the first things one learns about is Feynman diagrams: how they were first derived and how to use them practically. Explanations usually begin by attempting to calculate the scattering amplitude for a simple scalar particle interaction via the Feynman path integral formulation, looking something like

$$\langle q'', t'' | q', t' \rangle = \int \mathcal{D}q \exp \left[\int_{t'}^{t''} dt L(\dot{q}(t), q(t)) \right] \quad (4.1)$$

This integral is impossible to solve analytically in most cases. However, Feynman realized that one could Taylor expand the integrand of this integral and match the terms to specific particle interactions, order by order. He created the Feynman diagrams as a way to graphically represent these interactions in a clear way. The diagrams also serve as a method to return to the calculation of the scattering amplitudes by relating the parts of the diagram to pieces of the Taylor expanded integrand. Feynman wrote down several key rules for how to make this mapping and thereby find the amplitude. While these rules change somewhat depending on what types of particles and interactions one is dealing with, we will here enumerate the ones that are important for our calculation as listed in [16, 32].

1. Momentum labels: Label all the incoming and outgoing (external) momenta k_1, k_2, \dots, k_n . Label all internal momenta q_1, q_2, \dots, q_n . Put an arrow on or

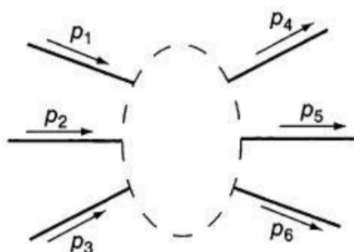


Figure 4.1: A generic Feynman diagram, with external lines labeled (internal lines not shown). Figure and caption taken from [32]

alongside each line to designate the positive flow of the momentum.

2. Propagators: For each internal line, write down the corresponding propagator term. Each of these propagators correspond to a particle, or more accurately, the path of a particle. For example, for a double squiggle as seen in fig. 5.1, which represents a graviton, the propagator takes the form $\frac{iP^{\alpha\beta\gamma\delta}}{q^2+i\epsilon}$, where $P^{\alpha\beta\gamma\delta}$ is defined in A.3.
3. Vertex factors: For each vertex between propagators, write down a vertex factor corresponding to the particle type of vertex. These vertices correspond to interaction points between the participating particles. They also usually have a coupling constant which determines how strong an interaction will be.
4. Conservation of energy/momentum: For each vertex, write down a delta function of the form $(2\pi)^4\delta^4(k_1+k_2+k_3)$, with positive momenta defined as coming *into* the vertex. This should make sure that momentum is conserved throughout the diagram.
5. Integration/Loops: Now integrate over each internal momenta. The differential should take the form $\frac{d^4q_i}{(2\pi)^4}$. The delta functions from momentum conservation should cancel out most of the integrals, unless there are loops. Since there can be an undefined amount of momenta flowing around a loop, all possible values for that momenta must be integrated over.
6. Cancel the delta function: Finally, there should be one remaining delta function of the form $(2\pi)^4\delta^4(p_1+p_2+\dots-p_n)$, which contains the overall momentum conservation for the diagram. Cancel this factor, and multiply the amplitude by i . The result should be the scattering amplitude \mathcal{M} for the diagram.

4.2 Changes in the Feynman Rules due to Massive Gravity

The propagators and vertex factors for the massless graviton were given in [5, 11] and then replicated in Appendix A for ease of reference. We then consulted a paper by Hinterbichler on massive gravity [19] to determine how these Feynman rules might change given a massive graviton. We found that while $(\tau_1, \tau_2, \tau_3, \tau_g)$ do not change form, the propagator for the graviton does. While the massless graviton propagator takes the form

$$\frac{i\frac{1}{2}[\eta^{\alpha\gamma}\eta^{\beta\delta} + \eta^{\alpha\delta}\eta^{\beta\gamma} - \frac{2}{D-2}\eta^{\alpha\beta}\eta^{\gamma\delta}]}{q^2 + i\epsilon} \quad (4.2)$$

in D dimensions, the massive graviton propagator takes the more complex form

$$\frac{i\frac{1}{2} \left[F_m^{\alpha\gamma}(q, m) F_m^{\beta\delta}(q, m) + F_m^{\alpha\delta}(q, m) F_m^{\beta\gamma}(q, m) - \frac{2}{D-1} F_m^{\alpha\beta}(q, m) F_m^{\gamma\delta}(q, m) \right]}{q^2 + i\epsilon} \quad (4.3)$$

where $F_m^{\alpha\beta}(q, m) = \eta^{\alpha\beta} + \frac{q^\alpha q^\beta}{m^2}$. We can see that in the limit $m \rightarrow 0$, the massive propagator does not smoothly return back to the massless propagator. Even if we ignore the singular terms, there is still a difference of a factor of $\frac{2}{D-1}$ instead of $\frac{2}{D-2}$. This is due to the fact that for this project, we chose to use the Fierz-Pauli theory of massive gravity instead of the Stückelberg theory. Although it has the detriment that the vDVZ discontinuity is present, the overall calculation is simplified because we do not have to calculate the additional interactions from the extra Stückelberg fields.

4.3 The Nonanalytic Component of the Scattering Matrix

A normal scattering amplitude in the massless graviton case will take the following:

$$M \sim \left(A + Bq^2 + \dots + \alpha\kappa^2 \frac{1}{q^2} + \beta_1\kappa^4 \ln(-q^2) + \beta_2\kappa^4 \frac{m}{\sqrt{-q^2}} + \dots \right) \quad (4.4)$$

The coefficients A, B, \dots correspond to the analytic components while the $\alpha, \beta_1, \beta_2, \dots$ correspond to the nonanalytic components. In this thesis, we will only analyze the nonanalytic terms of the scattering amplitude. This is due to the fact that analytic terms, when Fourier transformed will map to delta functions, which are purely local phenomena. We would only expect these terms to dominate in the very high energy regime, so in this effective field theory, we can ignore their contribution. We will instead focus on the nonanalytic terms which Fourier transform to sequential powers of $\frac{1}{r}$. In particular, the α term will yield the Newtonian potential, while β_1, β_2 terms will respectively yield the leading classical and quantum corrections to the Newtonian potential.

For the massive graviton case, the amplitude will look a bit different, but we will still only select the nonanalytic terms. We expect that we should again see the same $\alpha, \beta_1, \beta_2, \dots$ terms, but with different coefficients out front. These terms may also include an exponential decay due to the graviton mass turning the Newtonian potential to a Yukawa potential.

In this thesis, we will be examining 12 different diagrams (see figs 5.1, 6.2, 6.3, 6.1, 6.4, and 6.5) that contribute to this nonanalytic portion of the amplitude. Many

other diagrams yield only analytic contributions, so we will omit any discussion of them. The diagrams that do contribute to the nonanalytic amplitude are those which contain two or more propagating gravitons (except for the tree amplitude, which only has one).

Chapter 5

TREE LEVEL AMPLITUDES

5.1 Massless Graviton Interactions

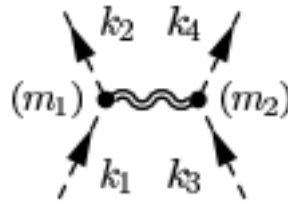
With the Feynman rules in hand, the calculation of the tree level diagram (see 5.1) is straightforward. It does not require any integration, but merely complex tensor algebra. To aid in this process, we utilize the Mathematica package Feyncalc which is built for reducing Einstein summation notation and solving Feynman integrals [28, 31]. We find the scattering amplitude to be

$$iM(q) = \tau_1^{\mu\nu}(k_1, k_2, m_1) \left[\frac{iP_{\mu\nu\alpha\beta}}{q^2} \right] \tau_1^{\alpha\beta}(k_3, k_4, m_2) \quad (5.1)$$

where $q = k_1 - k_2 = k_4 - k_3$. If we contract all indices, we get

$$iM(q) = \frac{i\kappa^2}{2q^2} \left[(k_1 \cdot k_4)(k_2 \cdot k_3) + (k_1 \cdot k_3)(k_2 \cdot k_4) - (k_1 \cdot k_2)(k_3 \cdot k_4) + m_2^2(k_1 \cdot k_2) + m_1^2(k_3 \cdot k_4) - 2m_1^2 m_2^2 \right] \quad (5.2)$$

In order to confirm this as the known result, we take the non-relativistic and zero velocity limit to yield the Newtonian potential. We define k_2 and k_4 in terms of k_1 , k_3 , and q ; divide by $\frac{1}{4E_1 E_3} = \frac{1}{4m_1 m_2}$; and set all dot products of external momenta equal to the product of their masses, e.g. $k_1 \cdot k_1 \rightarrow m_1^2$, $k_1 \cdot k_2 \rightarrow m_1^2$, $k_1 \cdot k_3 \rightarrow m_1 m_2$, etc. We also define $\kappa^2 = 32\pi G$. Given these approximations, we recover the much



1(a)

Figure 5.1: The Tree Level Diagram. Figure taken from [5]

simpler amplitude:

$$iM(q) = \frac{i32\pi G m_1 m_2}{8q^2} + \frac{i32\pi G q^2}{4q^2} = \frac{i4\pi G m_1 m_2}{q^2} + i4\pi G \quad (5.3)$$

We can now Fourier transform this amplitude to obtain the potential:

$$V(r) = \frac{G m_1 m_2}{r} - 4\pi G \delta^3(r) \quad (5.4)$$

However, we only care about non-local, long-distance classic interactions, so we can disregard the delta function (localized at a single point) to get the final solution which does match that of the Newtonian potential.

$$V(r) = \frac{G m_1 m_2}{r} \quad (5.5)$$

5.2 Massive Graviton Interactions

We then redo the calculation with the massive graviton propagator assuming a small mass of m for the graviton. The full expression remains nearly the same, only replacing the massless graviton propagator with the massive graviton propagator as defined in App. A:

$$iM(q) = \tau_1^{\mu\nu}(k_1, k_2, m_1) \left[\frac{iP m_{\mu\nu\alpha\beta}}{q^2 - m^2} \right] \tau_1^{\alpha\beta}(k_3, k_4, m_2) \quad (5.6)$$

Due to its complexities, we only replicate the non-relativistic limit of the amplitude here:

$$iM(q) = \frac{i\kappa^2}{q^2 - m^2} \left(\frac{q^4}{96m_1 m_2} + \frac{m_2 q^2}{48m_1} + \frac{m_1 q^2}{48m_2} + \frac{q^2}{8} + \frac{m_1 m_2}{6} \right) \quad (5.7)$$

We now change the form of the amplitude to reveal more clearly the parts that will become delta functions. We use the following relations:

$$\frac{q^2}{q^2 - m^2} = 1 + \frac{m^2}{q^2 - m^2} \quad (5.8)$$

$$\frac{q^4}{q^2 - m^2} = q^2 + m^2 + \frac{m^4}{q^2 - m^2} \quad (5.9)$$

and obtain:

$$\begin{aligned} iM(q) &= i\kappa^2 \left[\frac{1}{96m_1 m_2} \left(q^2 + m^2 + \frac{m^4}{q^2 - m^2} \right) \right. \\ &\quad \left. + \left(\frac{m_2}{48m_1} + \frac{m_1}{48m_2} + \frac{1}{8} \right) \left(1 + \frac{m^2}{q^2 - m^2} \right) + \frac{m_1 m_2}{6} \frac{1}{q^2 - m^2} \right] \\ &= \frac{i\kappa^2}{48m_1 m_2} \left[\frac{q^2}{2} + \left(\frac{m^2}{2} + m_2^2 + m_1^2 + 6m_1 m_2 \right) + \frac{1}{q^2 - m^2} \left(\frac{m^4}{2} + 8m_1^2 m_2^2 \right. \right. \\ &\quad \left. \left. + m^2 m_2^2 + m^2 m_1^2 + 6m^2 m_1 m_2 \right) \right] \quad (5.10) \end{aligned}$$

We can now Fourier transform this amplitude to obtain the potential:

$$V(r) = \frac{i2\pi G}{3m_1m_2} \left[\left(\frac{m^2}{2} + m_2^2 + m_1^2 + 6m_1m_2 \right) \delta^3(r) + \frac{1}{2} \delta^3(r) \right] + \frac{e^{-mr}}{4\pi r} \left(\frac{m^4}{2} + 8m_1^2m_2^2 + m^2m_2^2 + m^2m_1^2 + 6m^2m_1m_2 \right) \quad (5.11)$$

However, once again, we only care about non-local interactions, so we can disregard the delta function terms to get the final solution:

$$V(r) = \frac{Ge^{-mr}}{r} \left(\frac{4m_1m_2}{3} + \frac{m^2m_2}{6m_1} + \frac{m^2m_1}{6m_2} + m^2 + \frac{m^4}{12m_1m_2} \right) \quad (5.12)$$

We see that the term that would dominate in the limit of the graviton mass m being very small is a term that looks a lot like the original Newtonian potential. It has two small but key differences: an exponential decay with decay constant $1/m$ and an extra factor of $4/3$. The exponential decay term means that this potential now takes the form of a Yukawa potential, as expected. This potential is characteristic of any force mediated by a massive particle, see the weak force and W & Z bosons [22]. However, the factor of $4/3$ is due to the vDVZ discontinuity mentioned previously in Section 3.3. This is because we chose to use the original Pauli-Fierz theory instead of Stückelberg's method. While the newer method would have allowed us to have the smooth limit, it would have required us to account for many more particle interactions. We thus chose the simpler method for this calculation. However, it should still produce the same results either way.

Chapter 6

ONE-LOOP MODIFICATION (MASSLESS)

6.1 Techniques

After finishing the tree level calculations, we determined that we should rederive the gravitational potential at the one loop level for the massless graviton. Since this calculation had already been done several times, but with conflicting results, we believed that it would be good to redo it. As a reference, we followed a paper by Bjerrum-Bohr as well as another by Holstein which had both done this calculation or extremely similar ones [5, 21]. Since all the needed integrals had already been solved and recorded in these papers, this process went smoothly. In order to aid in contracting the many Einstein indices, we again utilized the Mathematica package FeynCalc. We coded up all the expressions for the propagators and vertex factors as well as the amplitudes for each diagram. We also replicated the results of the integrals from the two papers using FeynCalc's built in integral solving techniques. We created a simple program that took in each amplitude and output the solution in the desired format, contracting the indices and simplifying the expressions along the way. We also used several identities given in [5] that helped us eliminate many analytic terms from the start. In particular, these identities took the form

$$J_{\mu\nu\alpha}\eta^{\alpha\beta} = J_{\mu\nu}\eta^{\mu\nu} = I_{\mu\nu}\eta^{\mu\nu} = 0 \quad (6.1)$$

$$J_{\mu\nu\alpha}q^\alpha = -\frac{q^2}{2}J_{\mu\nu}, J_{\mu\nu}q^\nu = -\frac{q^2}{2}J_\mu, J_\mu q^\mu = -\frac{q^2}{2}J \quad (6.2)$$

$$I_{\mu\nu}q^\nu = -\frac{q^2}{2}I_\mu, I_\mu q^\mu = -\frac{q^2}{2}I \quad (6.3)$$

$$J_{\mu\nu\alpha}k^\alpha = \frac{1}{2}I_{\mu\nu}, J_{\mu\nu}k^\nu = \frac{1}{2}I_\mu, J_\mu k^\mu = \frac{1}{2}I \quad (6.4)$$

Through this procedure, we were able to derive each of the contributions to the gravitational potential from the diagrams. In all cases where the two previous papers that we referenced agreed, our result also confirmed theirs exactly [5, 21]. In the one case where there was one difference between the results of the two papers, our result matched that of [21], the newer paper.



Figure 6.1: The box and crossed box diagrams which contribute to the nonanalytic component of the potential. Figure and caption taken from [5].

6.2 Results

The Box and Crossed Box Diagrams

As given in [5], the uncontracted amplitudes for the box and cross box diagrams (see 6.1) are

$$iM_{2a} = \int \frac{d^4l}{(2\pi)^4} \tau_1^{\mu\nu}(k_1, k_1 + l, m_1) \tau_1^{\rho\sigma}(k_1 + l, k_2, m_1) \tau_1^{\alpha\beta}(k_3, k_3 - l, m_2) \tau_1^{\gamma\delta}(k_3 - l, k_4, m_2) \\ \times \left[\frac{i}{(k_1 + l)^2 - m_1^2} \right] \left[\frac{i}{(k_3 - l)^2 - m_2^2} \right] \left[\frac{iP_{\mu\nu\alpha\beta}}{l^2} \right] \left[\frac{iP_{\rho\sigma\gamma\delta}}{(l + q)^2} \right] \quad (6.5)$$

for the box and

$$iM_{2b} = \int \frac{d^4l}{(2\pi)^4} \tau_1^{\mu\nu}(k_1, k_1 + l, m_1) \tau_1^{\rho\sigma}(k_1 + l, k_2, m_1) \tau_1^{\gamma\delta}(k_3, k_4 + l, m_2) \tau_1^{\alpha\beta}(k_4 + l, k_4, m_2) \\ \times \left[\frac{i}{(k_1 + l)^2 - m_1^2} \right] \left[\frac{i}{(k_3 - l)^2 - m_2^2} \right] \left[\frac{iP_{\mu\nu\alpha\beta}}{l^2} \right] \left[\frac{iP_{\rho\sigma\gamma\delta}}{(l + q)^2} \right] \quad (6.6)$$

for the cross box. These two most complex diagrams require extra strategies of simplification before integration. We use the fact that only the lowest order non-analytic pieces contribute to eliminate portions of the integrals and eliminate all dependence on any integral more complex than the scalar box and cross integrals (as done in [5]). For example, we can simplify this integral

$$\int \frac{d^4l}{(2\pi)^4} \frac{l \cdot k_1}{l^2(l + q)^2((l + k_1)^2 - m_1^2)((l - k_3)^2 - m_2^2)} \\ = \frac{1}{2} \int \frac{d^4l}{(2\pi)^4} \frac{(l + k_1)^2 - l^2 - m_1^2}{l^2(l + q)^2((l + k_1)^2 - m_1^2)((l - k_3)^2 - m_2^2)} \quad (6.7)$$

into simply

$$\frac{1}{2} \int \frac{d^4l}{(2\pi)^4} \frac{1}{l^2(l + q)^2((l - k_3)^2 - m_2^2)} \quad (6.8)$$

because the l^2 term does not contribute to the non-analytic component. Similarly, we can turn

$$\begin{aligned} & \int \frac{d^4 l}{(2\pi)^4} \frac{l \cdot q}{l^2(l+q)^2((l+k_1)^2 - m_1^2)((l-k_3)^2 - m_2^2)} \\ &= \frac{1}{2} \int \frac{d^4 l}{(2\pi)^4} \frac{(l+q)^2 - l^2 - q^2}{l^2(l+q)^2((l+k_1)^2 - m_1^2)((l-k_3)^2 - m_2^2)} \end{aligned} \quad (6.9)$$

into this much simpler scalar integral

$$\frac{1}{2} \int \frac{d^4 l}{(2\pi)^4} \frac{q^2}{l^2(l+q)^2((l+k_1)^2 - m_1^2)((l-k_3)^2 - m_2^2)} \quad (6.10)$$

These simplifications are a simple example of the Passerino-Veltman decomposition which is described in detail in Section 7.2. They allow us to reduce these difficult integrals into less difficult integrals with few propagators and one scalar integral with four propagators. Using the integrals in Appendix B, and taking the nonrelativistic limit, we found that our results confirm those of Holstein and Bjerrum-Bohr et. al. [5, 21]:

$$\begin{aligned} M_{2a}(q) = G^2 m_1 m_2 & \left[\left(\frac{4m_1 m_2}{q^2} + 8 \left(\frac{m_1^2 + m_2^2}{m_1 m_2} \right) - 8 \right) L + 4(m_1 + m_2) S \right] \\ & - i4\pi G^2 m_1^2 m_2^2 \frac{L}{q^2} \sqrt{\frac{m_1 m_2}{s - s_0}} \end{aligned} \quad (6.11)$$

$$M_{2b}(q) = G^2 m_1 m_2 \left[\left(-\frac{4m_1 m_2}{q^2} - \frac{70}{3} \left(\frac{m_1^2 + m_2^2}{m_1 m_2} \right) - 8 \right) L - 4(m_1 + m_2) S \right] \quad (6.12)$$

where $L = \log(-q^2)$ and $S = \frac{\pi^2}{\sqrt{-q^2}}$. Adding these two terms together, we find the full amplitude for the box and crossed box diagrams to be

$$M_{2a+2b} = \frac{94}{3} G^2 m_1 m_2 \log q^2 - i4\pi G^2 m_1^2 m_2^2 \frac{L}{q^2} \sqrt{\frac{m_1 m_2}{s - s_0}} \quad (6.13)$$

where $s = (k_1 + k_3)^2$ is the square of the center of mass energy and $s_0 = (m_1 + m_2)^2$ is its threshold value. We note that the full amplitude does have an extra term as compared to [5], specifically the term with $s - s_0$. However, this term is present in [21], a more recent paper. This paper explains its presence as from the second order Born approximation and must thereby be subtracted off to find the correct correction to the Newtonian potential, producing

$$M_{2a+2b}(q) = \frac{94}{3} G^2 m_1 m_2 \log q^2 \quad (6.14)$$

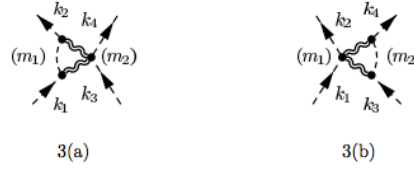


Figure 6.2: The set of triangle diagrams contributing to the scattering amplitude. Figure and caption taken from [5].

Fourier transforming the result gives us the potential due to these diagrams

$$V_{2a+2b}(r) = \frac{47}{3} \frac{G^2 m_1 m_2}{\pi r^3} \quad (6.15)$$

This is off by a negative sign from [5] (as all of the rest of the potentials will also be), but matches the potential derived in [21] exactly. This difference of a negative sign is simply due to a difference in convention for potentials.

The Triangle Diagrams

We next move onto the next set of diagrams: the triangle diagrams (as seen in 6.2). The uncontracted amplitudes take the form

$$M_{3a}(q) = \int \frac{d^4 l}{(2\pi)^4} \tau_1^{\mu\nu}(k_1, l + k_1, m_1) \tau_1^{\alpha\beta}(l + k_1, k_2, m_1) \tau_2^{\sigma\rho\gamma\delta}(k_3, k_4, m_2) \\ \times \left[\frac{iP_{\alpha\beta\gamma\delta}}{(l+q)^2} \right] \left[\frac{iP_{\mu\nu\sigma\rho}}{l^2} \right] \left[\frac{i}{((l+k_1)^2 - m_1^2)} \right] \quad (6.16)$$

$$M_{3b}(q) = \int \frac{d^4 l}{(2\pi)^4} \tau_1^{\sigma\rho}(k_3, k_3 - l, m_2) \tau_1^{\gamma\delta}(k_3 - l, k_4, m_2) \tau_2^{\mu\nu\alpha\beta}(k_1, k_2, m_1) \\ \times \left[\frac{iP_{\mu\nu\sigma\rho}}{l^2} \right] \left[\frac{iP_{\alpha\beta\gamma\delta}}{(l+q)^2} \right] \left[\frac{i}{((l-k_3)^2 - m_2^2)} \right] \quad (6.17)$$

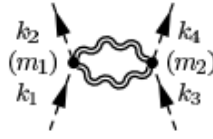
Unlike the box and crossed box diagrams, these diagrams have simple integrals as laid out in Appendix B. However, we are able to simplify the expression significantly through the use of the identity

$$P_{\gamma\delta\sigma\rho} P_{\alpha\beta\mu\nu} \tau^{\sigma\rho\mu\nu}(k_1, k_2, m_1) = \tau_{\gamma\delta\alpha\beta}(k_1, k_2, m_1) \quad (6.18)$$

Taking the nonrelativistic limit, we found that our results confirm those of [5] and [21]:

$$M_{3a}(q) = 8G^2 m_1 m_2 \left(\frac{7}{2} L + m_1 S \right) \quad (6.19)$$

$$M_{3b}(q) = 8G^2 m_1 m_2 \left(\frac{7}{2} L + m_2 S \right) \quad (6.20)$$



4(a)

Figure 6.3: The double-seagull contribution to the scattering amplitude. Figure and caption taken from [5].

where $L = \log(-q^2)$ and $S = \frac{\pi^2}{\sqrt{-q^2}}$. The Fourier transformed potential is thus

$$V_{3a+3b}(r) = \frac{4G^2 m_1 m_2 (m_1 + m_2)}{r^2} + \frac{28m_1 m_2 G^2}{\pi r^3} \quad (6.21)$$

The Double-Seagull Diagram

For the double-seagull diagram, the amplitude is as follows

$$M_{4a}(q) = \frac{1}{2!} \int \frac{d^4 l}{(2\pi)^4} \tau_2^{\alpha\beta\gamma\delta}(k_1, k_2, m_1) \tau_2^{\mu\nu\sigma\rho}(k_3, k_4, m_2) \left[\frac{iP_{\gamma\delta\sigma\rho}}{l^2} \right] \left[\frac{iP_{\alpha\beta\mu\nu}}{(l+q)^2} \right] \quad (6.22)$$

We again are able to use the simplifying identity from eq. 6.18. We also note that due to the symmetry of the diagram, there is a symmetry factor of $1/2!$. The resulting, contracted amplitude is

$$M_{4a}(q) = -44G^2 m_1 m_2 L \quad (6.23)$$

where $L = \log(-q^2)$. From this, a simply Fourier transform reveals the double-seagull diagram's correction to the potential

$$V_{4a}(r) = \frac{22G^2 m_1 m_2}{\pi r^3} \quad (6.24)$$

which agrees with the calculations in [5].

The Vertex Correction Diagrams

While there are more than four general vertex correction diagrams, the four shown in fig. 6.4 are the only ones which contribute to the nonanalytic portion of the scattering amplitude M . These figures can be divided into two classes: those with massive loops and those with purely graviton loops. For the massive loop diagrams

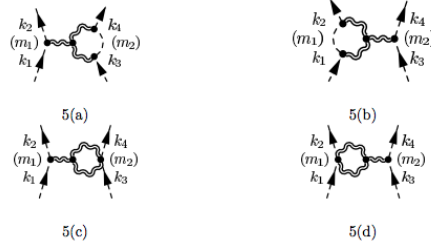


Figure 6.4: The class of the graviton vertex correction diagrams which yield non-analytic corrections to the potential. Figure and caption taken from [5].

(5a and 5b), the scattering amplitudes take the form

$$M_{5a}(q) = \int \frac{d^4l}{(2\pi)^4} \tau_1^{\alpha\beta}(k_1, k_2, m_1) \tau_1^{\mu\nu}(k_3, k_3 - l, m_2) \tau_1^{\rho\sigma}(k_3 - l, k_4, m_2) \tau_3^{(\gamma\delta)\lambda\kappa\phi\epsilon}(l, -q) \\ \times \left[\frac{iP_{\alpha\beta\gamma\delta}}{l^2} \right] \left[\frac{iP_{\mu\nu\sigma\rho}}{(l+q)^2} \right] \left[\frac{iP_{\lambda\kappa\phi\epsilon}}{q^2} \right] \left[\frac{i}{((l-k_3)^2 - m_2^2)} \right] \quad (6.25)$$

and

$$M_{5b}(q) = \int \frac{d^4l}{(2\pi)^4} \tau_1^{\alpha\beta}(k_1, l+k_1, m_1) \tau_1^{\mu\nu}(l+k_1, k_2, m_1) \tau_1^{\lambda\kappa}(k_3, k_4, m_2) \tau_3^{(\phi\epsilon)\gamma\delta\rho\sigma}(-l, q) \\ \times \left[\frac{iP_{\alpha\beta\gamma\delta}}{l^2} \right] \left[\frac{iP_{\mu\nu\sigma\rho}}{(l+q)^2} \right] \left[\frac{iP_{\phi\epsilon\lambda\kappa}}{q^2} \right] \left[\frac{i}{((l+k_1)^2 - m_1^2)} \right] \quad (6.26)$$

while the graviton loop diagrams (5c and 5d) take the form

$$M_{5c}(q) = \frac{1}{2!} \int \frac{d^4l}{(2\pi)^4} \tau_2^{\lambda\kappa\phi\epsilon}(k_3, k_4, m_2) \tau_1^{\alpha\beta}(k_1, k_2, m_1) \tau_3^{(\gamma\delta)\mu\nu\rho\sigma}(l, -q) \\ \times \left[\frac{iP_{\mu\nu\lambda\kappa}}{l^2} \right] \left[\frac{iP_{\sigma\rho\phi\epsilon}}{(l+q)^2} \right] \left[\frac{iP_{\alpha\beta\gamma\delta}}{q^2} \right] \quad (6.27)$$

and

$$M_{5d}(q) = \frac{1}{2!} \int \frac{d^4l}{(2\pi)^4} \tau_2^{\rho\sigma\mu\nu}(k_1, k_2, m_1) \tau_1^{\lambda\kappa}(k_3, k_4, m_2) \tau_3^{(\phi\epsilon)\alpha\beta\gamma\delta}(-l, q) \\ \times \left[\frac{iP_{\mu\nu\gamma\delta}}{l^2} \right] \left[\frac{iP_{\sigma\rho\alpha\beta}}{(l+q)^2} \right] \left[\frac{iP_{\lambda\kappa\phi\epsilon}}{q^2} \right] \quad (6.28)$$

The second set of diagrams also have a symmetry factor of $1/2!$. These diagrams have the second most propagators (second only to the box and crossed box diagrams) and are thereby some of the more difficult ones to solve. However, we were able to

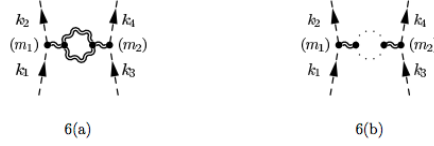


Figure 6.5: The vacuum polarization diagrams which contribute to the potential. Note that there exists a ghost diagram along with the graviton loop. Figure and caption taken from [5].

find the nonrelativistic, contracted amplitudes

$$M_{5a}(q) = G^2 m_1 m_2 \left(\frac{5}{3} L + 2m_1 S \right) \quad (6.29)$$

$$M_{5b}(q) = G^2 m_1 m_2 \left(\frac{5}{3} L + 2m_2 S \right) \quad (6.30)$$

$$M_{5c+5d}(q) = \frac{52}{3} G^2 m_1 m_2 L \quad (6.31)$$

where $L = \log(-q^2)$ and $S = \frac{\pi^2}{\sqrt{-q^2}}$. Adding the first two similar terms together, we find

$$M_{5a+5b}(q) = 2G^2 m_1 m_2 \left(\frac{5}{3} L + (m_1 + m_2) S \right) \quad (6.32)$$

$$M_{5c+5d}(q) = \frac{52}{3} G^2 m_1 m_2 L \quad (6.33)$$

Once again Fourier transforming to yield the potential, we find

$$V_{5a+5b} = \frac{G^2 m_1 m_2 (m_1 + m_2)}{r^2} - \frac{5}{3} \frac{G^2 m_1 m_2}{\pi r^3} \quad (6.34)$$

and

$$V_{5c+5d} = -\frac{26}{3} \frac{G^2 m_1 m_2}{\pi r^3} \quad (6.35)$$

These results again agree with the calculations in the paper [5].

The Vacuum Polarization Diagrams

Finally, we examine the effect of the two vacuum polarization diagrams, both from a pure graviton loop as well as a ghost loop (see fig. 6.5). We again note that there should be a vertex factor of $1/2!$ due to the symmetry of the diagrams. Conveniently, we are able to use an effective Lagrangian calculated by 't Hooft and Veltman [15, 34, 35]

$$\mathcal{L} = -\frac{1}{16\pi^2} \log q^2 \left(\frac{1}{120} R^2 + \frac{7}{20} R_{\mu\nu} R^{\mu\nu} \right) \quad (6.36)$$

to find a vacuum polarization tensor which is given by

$$\begin{aligned} \hat{\Pi}_{\alpha\beta,\gamma\delta} = & -\frac{2G}{\pi} \log(-q^2) \left[\frac{21}{120} q^4 I_{\alpha\beta,\gamma\delta} + \frac{23}{120} q^4 \eta_{\alpha\beta} \eta_{\gamma\delta} \right. \\ & - \frac{23}{120} q^2 (\eta_{\alpha\beta} q_\gamma q_\delta + \eta_{\gamma\delta} q_\alpha q_\beta) - \frac{21}{240} q^2 (q_\alpha q_\delta \eta_{\beta\gamma} \\ & \left. + q_\beta q_\delta \eta_{\alpha\gamma} + q_\beta q_\gamma \eta_{\alpha\delta}) + \frac{11}{30} q_\alpha q_\beta q_\gamma q_\delta \right] \end{aligned} \quad (6.37)$$

We can then use this vacuum polarization tensor to easily find the amplitude

$$M_{6ab}(q) = \tau_1^{\sigma\rho}(k_1, k_2, m_1) \left[\frac{iP_{\sigma\rho\phi\epsilon}}{q^2} \right] \Pi^{\phi\epsilon\mu\nu} \left[\frac{iP_{\mu\nu\lambda\kappa}}{q^2} \right] \tau_1^{\lambda\kappa}(k_3, k_4, m_2) \quad (6.38)$$

Contracting and taking the nonrelativistic approximation, we get

$$M_{6ab}(q) = -\frac{43}{15} G^2 m_1 m_2 L \quad (6.39)$$

where $L = \log(-q^2)$. Taking the final Fourier transform, we find the expected result

$$V_{6a+6b}(r) = \frac{43}{30} \frac{G^2 m_1 m_2}{\pi r^3} \quad (6.40)$$

just as seen in [5].

6.3 Analysis of Full Potential

We can add up all of the contributions to the potential from each of the diagrams to find the full gravitational potential at one loop order

$$V(r) = \frac{Gm_1 m_2}{r} \left[1 + 3 \frac{G(m_1 + m_2)}{r} + \frac{41}{10\pi} \frac{G\hbar}{r^2} \right] \quad (6.41)$$

We note the addition of the factor of \hbar on the third term is added to make units work correctly, which was until now ignored.

We see that that these terms seem to follow our expectations from Section 2.2 according to simple order counting methods. The first term is obviously the Newtonian potential as discussed above, which is at order 0 in the Post-Newtonian (PN) approximation method or order 1 in the Post-Minkowski (PM) approximation method due to its singular factor of G . The second two terms both share a factor of G^2 , which puts them both at PM order 2. However, it is more difficult to determine their order on the PN scale. In fact, the second term exactly corresponds to the first term seen in a PN calculation via numerical relativity [23]. Due to this fact, it is usually denoted the classical or Post-Newtonian term. However, the third term is not so

easy to classify since it cannot be easily matched to any regular Post-Newtonian approximations. Instead, this term is the new contribution of this effective field theoretic calculation. We can thus interpret this aptly named "quantum term" to encapsulate all orders of v^2 into its one term (see the first row in fig. 2.2). However, due to an extra factor of $\frac{GM}{r}$ as well as one of \hbar which suppress its contribution, in this regime, this term is actually much smaller than the classical term even though they are technically at the same PM order. Thus, while theoretically interesting, the small value usually renders the quantum term impractical for common calculations, since the classical term(s) will dominate in most realms of interest.

Chapter 7

INTEGRATION WITH A MASSIVE GRAVITON

Unfortunately, the addition of the graviton mass on the graviton propagator meant that all of the original integrals used in the massless graviton calculations no longer held. We thus needed to calculate all of the necessary integrals in order to find the correct expressions for the amplitudes. These integrals took 4 different forms depending on how many propagators were being integrated over and how many indices they had. We labelled them as A , B , C , or D integrals if they had 1, 2, 3, or 4 propagators respectively, as seen below:

$$A_0 = \int \frac{d^4\ell}{(2\pi)^4} \frac{1}{(\ell^2 - m_1^2)} \quad (7.1)$$

$$B_0 = \int \frac{d^4\ell}{(2\pi)^4} \frac{1}{(\ell^2 - m_1^2)((\ell + q)^2 - m_2^2)} \quad (7.2)$$

$$C_0 = \int \frac{d^4\ell}{(2\pi)^4} \frac{1}{(\ell^2 - m_1^2)((\ell + q)^2 - m_2^2)((\ell + k_1)^2 - m_3^2)} \quad (7.3)$$

$$D_0 = \int \frac{d^4\ell}{(2\pi)^4} \frac{1}{(\ell^2 - m_1^2)((\ell + q)^2 - m_2^2)((\ell + k_1)^2 - m_3^2)((\ell + k_2)^2 - m_4^2)} \quad (7.4)$$

At times, we also equivalently refer to them as tadpole, bubble, triangle and box integrals. This labelling system refers to the types of diagrams that one would expect these integrals to originate from.

Similarly, if they are scalar integrals as shown above, they have have a subscript 0, while integral tensors will have indices to match their rank as seen below:

$$B_0 = \int \frac{d^4\ell}{(2\pi)^4} \frac{1}{(\ell^2 - m_1^2)((\ell + q)^2 - m_2^2)} \quad (7.5)$$

$$B^\mu = \int \frac{d^4\ell}{(2\pi)^4} \frac{\ell^\mu}{(\ell^2 - m_1^2)((\ell + q)^2 - m_2^2)} \quad (7.6)$$

$$B^{\mu\nu} = \int \frac{d^4\ell}{(2\pi)^4} \frac{\ell^\mu \ell^\nu}{(\ell^2 - m_1^2)((\ell + q)^2 - m_2^2)} \quad (7.7)$$

...

This method of defining integrals is characteristic of the Passarino-Veltman decomposition technique which we will describe in detail in Section 7.2

7.1 Scalar Integrals

Feyncalc already had the solutions for the A_0 and B_0 integrals programmed into their code base. We were thus able to utilize these solutions and separated out the nonanalytic portion of each of them. We coded this simpler version of them, as seen in Appendix C.1, into our program.

Unfortunately, Feyncalc did not have the expressions for C_0 or D_0 , so we had to look elsewhere. We found several resources that had solved these integrals for various cases [13, 14, 30], however none of these solved the integrals in the most general case which is what we needed for our project. Ultimately, we did find one source that did have a more general solution for both [10]. Devaraj and Stuart's solution for C_0 is valid when the kinematic determinant vanishes

$$\mathcal{D} = p_1^2 p_2^2 - (p_1 \cdot p_2)^2 = 0 \quad (7.8)$$

While they found two solutions depending on which combinations of p_1 and p_2 made the determinant vanish, we were able to determine that our integrals only followed the format of the second, allowing us to use and record only one solution. This paper found a solution for D_0 in a similar fashion, requiring the kinematic determinant to vanish

$$\begin{aligned} \mathcal{D} = p_1^2 p_2^2 p_3^2 - p_1^2 (p_2 \cdot p_3)^2 - p_2^2 (p_1 \cdot p_3)^2 - p_3^2 (p_1 \cdot p_2)^2 \\ + 2(p_1 \cdot p_2)(p_1 \cdot p_3)(p_2 \cdot p_3) = 0 \end{aligned} \quad (7.9)$$

This time we utilized two of the three solutions, as recorded in Appendix C.3, for the box and crossed box diagrams. Thus we were able to find and use expressions for each of the scalar integrals that we needed.

7.2 Passarino-Veltman Decomposition

The Passarino-Veltman decomposition technique allows one to take advantage of the particular form of tensor integrals from Feynman diagrams and simplify them into an expression of the composite scalar integrals. This technique is applicable for all integrals with indices, regardless of the number of propagators or indices. It is also remarkably simple and adaptable compared to the original methods of solving these integrals, which would require returning back to dimensional regularization and other more difficult techniques. The process of decomposing can be divided up into several easy steps

First, check that your integral takes the form

$$\int \frac{d^4\ell}{(2\pi)^4} \frac{D(\ell, p_1, \dots, m_1, \dots)}{(\ell^2 - m_1^2)((\ell \pm p_1) - m_2^2) \dots ((\ell \pm p_n) - m_{n+1}^2)} \quad (7.10)$$

where $n \in \mathbb{R}$ and $D(\ell, p_1, \dots, m_1, \dots)$ is a general function of the momenta and masses. Take the function $D^{\mu_1 \dots \mu_n}$ and decompose it into the form

$$\alpha_0 + \alpha_1^{\mu_1} \ell_{\mu_1} + \alpha_2^{\mu_1 \mu_2} \ell_{\mu_1} \ell_{\mu_2} + \dots + \alpha_2^{\mu_1 \dots \mu_m} \ell_{\mu_1} \dots \ell_{\mu_m} + \ell^2 \left(\beta_0 + \beta_1^{\mu_1} \ell_{\mu_1} + \dots + \beta_2^{\mu_1 \dots \mu_m} \ell_{\mu_1} \dots \ell_{\mu_m} \right) + \dots, \quad (7.11)$$

separating each term depending on its ℓ dependence.

Let us first examine a term with a singular ℓ^μ . Dot ℓ with one of the momenta $\pm p_i$.

This term

$$\int \frac{d^4\ell}{(2\pi)^4} \frac{(\ell \cdot p_i)}{(\ell^2 - m_1^2)((\ell \pm p_1) - m_2^2) \dots ((\ell \pm p_n) - m_n^2)} \quad (7.12)$$

is equal to

$$\int \frac{d^4\ell}{(2\pi)^4} \frac{\pm \frac{1}{2} [(\ell \pm p_i)^2 - \ell^2 - p_i^2]}{(\ell^2 - m_1^2)((\ell \pm p_1) - m_2^2) \dots ((\ell \pm p_n) - m_n^2)} \quad (7.13)$$

If we put it in the form

$$\int \frac{d^4\ell}{(2\pi)^4} \frac{\pm \frac{1}{2} [((\ell \pm p_i)^2 - m_i^2) - (\ell^2 - m_1^2) + (m_i^2 - p_i^2 - m_1^2)]}{(\ell^2 - m_1^2)((\ell \pm p_1) - m_2^2) \dots ((\ell \pm p_n) - m_n^2)} \quad (7.14)$$

then we can see that many of the pieces should cancel. The first set of terms should cancel out the i th propagator, leaving a scalar integral with one less propagator. The second set of terms will cancel out the first propagator and similarly leave one less propagator. The third set of terms, which serves as a catchall, will simply leave a scalar integral behind. This results in

$$\begin{aligned} & \pm \frac{1}{2} \int \frac{d^4\ell}{(2\pi)^4} \frac{1}{(\ell^2 - m_1^2) \dots ((\ell \pm p_{i-1}) - m_i^2)((\ell \pm p_{i+1}) - m_{i+2}^2) \dots ((\ell \pm p_n) - m_n^2)} \\ & \mp \frac{1}{2} \int \frac{d^4\ell}{(2\pi)^4} \frac{1}{((\ell \pm p_1) - m_2^2) \dots ((\ell \pm p_n) - m_n^2)} \\ & \pm \frac{1}{2} \int \frac{d^4\ell}{(2\pi)^4} \frac{(m_i^2 - p_i^2 - m_1^2)}{(\ell^2 - m_1^2)((\ell \pm p_1) - m_2^2) \dots ((\ell \pm p_n) - m_n^2)} \end{aligned} \quad (7.15)$$

Now, since this is an integral of a tensor, we know that the solution of the integral must also be a tensor, using only the momenta available to it from the integral as

well as the metric η . This means that the solution to this integral must take the form

$$\int \frac{d^4\ell}{(2\pi)^4} \frac{\ell^\mu}{(\ell^2 - m_1^2)((\ell \pm p_1) - m_2^2)\dots((\ell \pm p_n) - m_n^2)} = A_1 p_1^\mu + \dots + A_n p_n^\mu \quad (7.16)$$

If we dot this with p_i , we can set this equal to the expression that we got from above and solve for one of the A_i coefficients. We can repeat this process for each of the p_i 's to get a system of n equations and n variables and thereby solve for all of the A coefficients.

While we have shown this process for any rank one integral (one index), it is very similar for integrals with more indices. The only difference is that one needs to take into account $\eta^{\mu\nu}$ on both sides of the equation. This is an additional way to cancel terms. We begin with

$$\int \frac{d^4\ell}{(2\pi)^4} \frac{\eta_{\mu\nu} \ell^\mu \ell^\nu}{(\ell^2 - m_1^2)((\ell \pm p_1) - m_2^2)\dots((\ell \pm p_n) - m_n^2)} \quad (7.17)$$

which can be put into the form

$$\int \frac{d^4\ell}{(2\pi)^4} \frac{(\ell^2 - m_1) + m_1}{(\ell^2 - m_1^2)((\ell \pm p_1) - m_2^2)\dots((\ell \pm p_n) - m_n^2)}. \quad (7.18)$$

The first term can then cancel with the first propagator, leaving

$$\begin{aligned} & \frac{1}{2} \int \frac{d^4\ell}{(2\pi)^4} \frac{1}{((\ell \pm p_1) - m_2^2)\dots((\ell \pm p_n) - m_n^2)} \\ & + \frac{1}{2} \int \frac{d^4\ell}{(2\pi)^4} \frac{m_1^2}{(\ell^2 - m_1^2)((\ell \pm p_1) - m_2^2)\dots((\ell \pm p_n) - m_n^2)} \end{aligned} \quad (7.19)$$

This expanded method lowers the rank of the resultant integrals by one each time (it does not always produce scalar integrals right away).

While this method is reasonably simple, it does become computationally intensive as the number of indices and momenta increases. Since it must take into account all permutations of the momenta and indices, and then solve the system of equations, the amount of computational time and power required grows exponentially.

All of the integrals that we solved were coded into the Mathematica notebook for future use. We also recorded them in Appendix C. Due to the long expressions for the triangle integrals, we chose to only record the Taylor expanded, highest order terms.

7.3 Tensor Integrals

The goal for all of these tensor integrals was to reduce them into expressions of the composite scalar integrals. Unfortunately, FeynCalc does not have a good internal method of doing this reduction. However, there is additional package called FeynHelpers which can also be downloaded. This package uses FeynCalc language and functions to interface with two other Mathematica packages, Package-X and FIRE, which are specifically built for solving integrals with propagators. With this combination of resources, we were able to decompose all of the bubble tensor integrals and the first three triangle tensor integrals. However, when attempting to decompose the last two triangle integrals, the computer that was being used ran out of available memory and could not complete the solution.

After running into these issues, we attempted to use the Passarino-Veltman decomposition technique to solve the last few integrals that we needed. We went through the process described in Section 7.2 and were able to decompose the $C^{\mu\nu\alpha\beta}$ integral. However, solving the $C^{\mu\nu\alpha\beta\gamma}$ integral required finding the solution to a general system of 12 equations for 12 variables or equivalently inverting a general 12x12 matrix. This once again made the available computer run out of memory since it used at least 12 GB of data. However, we realized that this integral was only required for the box and crossed box diagram. Because of this, we decided to change our focus as seen in Chapter 8.

ONE-LOOP MODIFICATION (MASSIVE)

8.1 Classical vs Quantum

Since we expect the diagrams to still produce the same q dependence, merely with extra factors, we expect that the diagrams should still split between those that contribute to both the classical and quantum term and those that only contribute to the quantum term. In particular, we expect the triangle diagrams (Fig 6.2) and the first two vertex correction diagrams (Fig 6.4) should still contribute to the classical portion. As mentioned in Section 6.3, the classical term should dominate the quantum term. In addition, although we were unable to solve the $C^{\mu\nu\alpha\beta\gamma}$ term, it is only used for the box and crossed box diagrams. Because of this, we decided to focus on deriving the results for the more relevant classical portion. However, since we had already made some progress on the other diagrams, we still relate what we have done in Section 8.5.

8.2 Techniques

In order to eliminate copy errors, we created a Mathematica pipeline to process the amplitudes. This pipeline takes in the uncontracted amplitude expressions as well as all the integral solutions. It uses various FeynCalc functions, such as Contract, Collect2 and Simplify to simplify the answers. It then applies the function ScalarProductCancel which reduces the number of the necessary integrals by canceling out propagators whenever possible. We next apply the integral solutions, take the nonrelativistic limit and simplify the ensuing expressions once again. The resulting expressions are long and have complicated dependence on q . In order to simplify this, we first Taylor expand with respect to the tiny graviton mass. We then Taylor expand with respect to the transferred momentum q , which we expect to be small, but not as small as the graviton mass m . The expressions shown below have the lowest order contributions of both the classical and quantum portions. We also include any other low order terms that are dependent on the graviton mass.

8.3 Results for Classical Diagrams

After confirming all the massless results, we begin the massive case for the diagrams that contribute to the classical potential term. Since the only Feynman rules that

change are the graviton propagators, we see that the new uncontracted amplitudes are simply as shown in the sections below.

The Triangle Diagrams

With only minor changes from the previous triangle diagram amplitudes (see 6.2), the new massive graviton amplitudes take the form

$$M_{3a}(q) = \int \frac{d^4l}{(2\pi)^4} \tau_1^{\mu\nu}(k_1, l + k_1, m_1) \tau_1^{\alpha\beta}(l + k_1, k_2, m_1) \tau_2^{\sigma\rho\gamma\delta}(k_3, k_4, m_2) \\ \times \left[\frac{iPm_{\alpha\beta\gamma\delta}}{(l+q)^2 - m^2} \right] \left[\frac{iPm_{\mu\nu\sigma\rho}}{l^2 - m^2} \right] \left[\frac{i}{((l+k_1)^2 - m_1^2)} \right] \quad (8.1)$$

$$M_{3b}(q) = \int \frac{d^4l}{(2\pi)^4} \tau_1^{\sigma\rho}(k_3, k_3 - l, m_2) \tau_1^{\gamma\delta}(k_3 - l, k_4, m_2) \tau_2^{\mu\nu\alpha\beta}(k_1, k_2, m_1) \\ \times \left[\frac{iPm_{\mu\nu\sigma\rho}}{l^2 - m^2} \right] \left[\frac{iPm_{\alpha\beta\gamma\delta}}{(l+q)^2 - m^2} \right] \left[\frac{i}{((l-k_3)^2 - m_2^2)} \right] \quad (8.2)$$

Once this amplitude is run through the Mathematica pipeline, we get the following expression for the contracted amplitude. This expression is only the nonanalytic terms after taylor expanding with respect to both m and q as well as taking the nonrelativistic approximation.

$$iM_{3a} = \frac{i16G^2}{135q^2} \left[1023m^2m_1m_2 \log\left(-\frac{m^2}{q^2}\right) - 598m^2m_1m_2 \right] + \frac{iG^2}{270m_1m_2} \left[2142m^2m_1^2 \right. \\ \left. - 27760m_2^2m_1^2 + 11592m^2m_1m_2 - 68m^2m_2^2 \right] \log\left(-\frac{m^2}{q^2}\right) \quad (8.3)$$

$$iM_{3b} = \frac{i16G^2}{135q^2} \left[1023m^2m_1m_2 \log\left(-\frac{m^2}{q^2}\right) - 598m^2m_1m_2 \right] + \frac{iG^2}{270m_1m_2} \left[2142m^2m_1^2 \right. \\ \left. - 27760m_2^2m_1^2 + 11592m^2m_1m_2 - 68m^2m_2^2 \right] \log\left(-\frac{m^2}{q^2}\right) \quad (8.4)$$

Adding the two disparate equations, we get the full amplitude from the two triangle diagrams

$$iM_{3a+3b} = \frac{i32G^2}{135q^2} \left[1023m^2m_1m_2 \log\left(-\frac{m^2}{q^2}\right) - 598m^2m_1m_2 \right] + \frac{iG^2}{135m_1m_2} \left[2142m^2m_1^2 \right. \\ \left. - 27760m_2^2m_1^2 + 11592m^2m_1m_2 - 68m^2m_2^2 \right] \log\left(-\frac{m^2}{q^2}\right) \quad (8.5)$$

We here note that $\log\left(-\frac{m^2}{q^2}\right)$ can be decomposed into $\log(m^2) - \log(-q^2)$. Since $\log(m^2)$ is actually only an analytic contribution, we remove it from the second set

of terms

$$iM_{3a+3b} = \frac{i32G^2}{135q^2} \left[-1023m^2m_1m_2 \log\left(-\frac{m^2}{q^2}\right) - 598m^2m_1m_2 \right] - \frac{iG^2}{135m_1m_2} \left[2142m^2m_1^2 \right. \\ \left. - 27760m_2^2m_1^2 + 11592m^2m_1m_2 - 68m^2m_2^2 \right] \log(-q^2) \quad (8.6)$$

We can then Fourier transform the expression to find their contribution to the potential

$$V_{3a+3b} = \frac{10912G^2m^2m_1m_2}{45} \int \frac{d^3q}{(2\pi)^3} e^{iq \cdot r} \frac{\log(-q^2)}{q^2} - \frac{4784}{135\pi} \frac{G^2m^2m_1m_2}{r} \\ + \frac{G^2}{135m_1m_2\pi r^3} \left[1071m^2m_1^2 - 13880m_2^2m_1^2 + 5796m^2m_1m_2 - 34m^2m_2^2 \right] \quad (8.7)$$

The Classical Vertex Correction Diagrams

We now specifically select out the two vertex correction diagrams (see 5.ab in 6.4) that contribute to the classical term in the potential. The uncontracted amplitude takes the form

$$M_{5a}(q) = \int \frac{d^4l}{(2\pi)^4} \tau_1^{\alpha\beta}(k_1, k_2, m_1) \tau_1^{\mu\nu}(k_3, k_3 - l, m_2) \tau_1^{\rho\sigma}(k_3 - l, k_4, m_2) \tau_3^{(\gamma\delta)\lambda\kappa\phi\epsilon}(l, -q) \\ \times \left[\frac{iPm_{\alpha\beta\gamma\delta}}{l^2 - m^2} \right] \left[\frac{iPm_{\mu\nu\sigma\rho}}{(l+q-m^2)^2} \right] \left[\frac{iPm_{\lambda\kappa\phi\epsilon}}{q^2 - m^2} \right] \left[\frac{i}{((l-k_3)^2 - m_2^2)} \right] \quad (8.8)$$

$$M_{5b}(q) = \int \frac{d^4l}{(2\pi)^4} \tau_1^{\alpha\beta}(k_1, l+k_1, m_1) \tau_1^{\mu\nu}(l+k_1, k_2, m_1) \tau_1^{\lambda\kappa}(k_3, k_4, m_2) \tau_3^{(\phi\epsilon)\gamma\delta\rho\sigma}(-l, q) \\ \times \left[\frac{iPm_{\alpha\beta\gamma\delta}}{l^2 - m^2} \right] \left[\frac{iPm_{\mu\nu\sigma\rho}}{(l+q)^2 - m^2} \right] \left[\frac{iPm_{\phi\epsilon\lambda\kappa}}{q^2 - m^2} \right] \left[\frac{i}{((l+k_1)^2 - m_1^2)} \right] \quad (8.9)$$

After we contract and simplify in the Mathematica pipeline, we get the following nonrelativistic amplitudes

$$iM_{5a} = \frac{iG^2}{540m^4(q^2 - m^2)} \left[-26616m^6m_1m_2 - 46852m^6m_1m_2 \log\left(-\frac{m^2}{q^2}\right) \right. \\ \left. + \left[240m_1m_2^7 + 530m^2m_1m_2^5 + 405m_2^8 + 1620m^2m_2^6 - 1085m^6m_1m_2 \right. \right. \\ \left. \left. - 240m^6m_2^2 + 615m^4m_1m_2^3 + 1665m^4m_2^4 \right] \log\left(\frac{m_2^2}{m^2}\right) \right]$$

$$\begin{aligned}
& + \left[7600m^6 m_1 m_2 - 2720m^4 m_1 m_2^3 \right] \log \left(-\frac{m^2}{m_2^2} \right) \\
& - \left[2680m^6 m_1 m_2 - 2880m^4 m_1 m_2^3 \right] \log \left(\frac{m^2}{m_2^2} \right)
\end{aligned} \tag{8.10}$$

$$\begin{aligned}
iM_{5b} = & -\frac{iG^2}{540m^4 (q^2 - m^2)} \left[26616m^6 m_1 m_2 + 46852m^6 m_1 m_2 \log \left(-\frac{m^2}{q^2} \right) \right. \\
& - \left[405m_1^8 - 240m_1^7 m_2 - 1620m^2 m_1^6 - 530m^2 m_1^5 m_2 + 1085m^6 m_1 m_2 \right. \\
& \quad \left. \left. + 240m^6 m_1^2 - 1665m^4 m_1^4 - 615m^4 m_1^3 m_2 \right] \log \left(\frac{m_1^2}{m^2} \right) \right. \\
& - \left[7600m^6 m_1 m_2 - 2720m^4 m_1^3 m_2 \right] \log \left(-\frac{m^2}{m_1^2} \right) \\
& \left. + \left[2680m^6 m_1 m_2 - 2880m^4 m_1^3 m_2 \right] \log \left(\frac{m^2}{m_1^2} \right) \right]
\end{aligned} \tag{8.11}$$

Let us now add the two amplitudes and determine what terms may cancel or add. We note that the terms with $\log \left(-\frac{m^2}{m_i^2} \right)$ will be imaginary since the masses are real and positive. We can thus eliminate them from our amplitude as we did before in 6.2. We also flip some of the logs for more clarity.

$$\begin{aligned}
iM_{5a+5b} = & \frac{iG^2}{540m^4 (q^2 - m^2)} \left[-53232m^6 m_1 m_2 - 93704m^6 m_1 m_2 \log \left(-\frac{m^2}{q^2} \right) \right. \\
& + \left[240m_1 m_2^7 + 530m^2 m_1 m_2^5 + 405m_2^8 + 1620m^2 m_2^6 - 1085m^6 m_1 m_2 \right. \\
& \quad \left. - 240m^6 m_2^2 + 615m^4 m_1 m_2^3 + 1665m^4 m_2^4 + 2680m^6 m_1 m_2 \right. \\
& \quad \left. - 2880m^4 m_1 m_2^3 \right] \log \left(\frac{m_2^2}{m^2} \right) \\
& + \left[405m_1^8 - 240m_1^7 m_2 - 1620m^2 m_1^6 - 530m^2 m_1^5 m_2 + 1085m^6 m_1 m_2 + \right. \\
& \quad \left. + 240m^6 m_1^2 - 1665m^4 m_1^4 - 615m^4 m_1^3 m_2 \right. \\
& \quad \left. - 2880m^4 m_1^3 m_2 \right] \log \left(\frac{m_1^2}{m^2} \right) \left. \right]
\end{aligned} \tag{8.12}$$

We can now Fourier transform this simplified expression to get the potential

$$\begin{aligned}
V_{5a+5b} = & \frac{23426G^2m^2m_1m_2}{135} \int \frac{d^3q}{(2\pi)^3} e^{iq \cdot r} \frac{\log(-q^2)}{(q^2 - m^2)} - \frac{1344}{452\pi} \frac{G^2m^2m_1m_2}{r} \\
& - \frac{1109}{45\pi} \frac{G^2m^2m_1m_2e^{-mr}}{r} + \frac{1}{4\pi} \frac{G^2e^{-mr}}{r} \left[\left[240m_1m_2^7 + 530m^2m_1m_2^5 \right. \right. \\
& + 405m_2^8 + 1620m^2m_2^6 - 1085m^6m_1m_2 - 240m^6m_2^2 + 615m^4m_1m_2^3 \\
& + 1665m^4m_2^4 + 2680m^6m_1m_2 - 2880m^4m_1m_2^3 \left. \right] \log\left(\frac{m_2^2}{m^2}\right) \\
& + \left[405m_1^8 - 240m_1^7m_2 - 1620m^2m_1^6 - 530m^2m_1^5m_2 + 1085m^6m_1m_2 \right. \\
& + 240m^6m_1^2 - 1665m^4m_1^4 - 615m^4m_1^3m_2 + 2680m^6m_1m_2 \\
& \left. \left. - 2880m^4m_1^3m_2 \right] \log\left(\frac{m_1^2}{m^2}\right) \right] \quad (8.13)
\end{aligned}$$

8.4 Classical Discussion

We can first begin by adding all of the different contributions to the classical potential together

$$\begin{aligned}
V_{clas} = & -\frac{8816}{135\pi} \frac{G^2m^2m_1m_2}{r} - \frac{1109}{45\pi} \frac{G^2m^2m_1m_2e^{-mr}}{r} \\
& + \frac{1}{4\pi} \frac{G^2e^{-mr}}{r} \left[\left[240m_1m_2^7 + 530m^2m_1m_2^5 + 405m_2^8 + 1620m^2m_2^6 \right. \right. \\
& - 1085m^6m_1m_2 - 240m^6m_2^2 + 615m^4m_1m_2^3 \\
& + 1665m^4m_2^4 + 2680m^6m_1m_2 - 2880m^4m_1m_2^3 \left. \right] \log\left(\frac{m_2^2}{m^2}\right) \\
& + \left[405m_1^8 - 240m_1^7m_2 - 1620m^2m_1^6 - 530m^2m_1^5m_2 + 1085m^6m_1m_2 \right. \\
& + 240m^6m_1^2 - 1665m^4m_1^4 - 615m^4m_1^3m_2 + 2680m^6m_1m_2 \\
& \left. \left. - 2880m^4m_1^3m_2 \right] \log\left(\frac{m_1^2}{m^2}\right) \right] \\
& + \frac{G^2}{135m_1m_2\pi r^3} \left[1071m^2m_1^2 - 13880m_2^2m_1^2 + 5796m^2m_1m_2 - 34m^2m_2^2 \right] \quad (8.14)
\end{aligned}$$

However, the last term is dependent on $\frac{1}{r^3}$, and is therefore a quantum term. We can thus ignore this term for this analysis of the classical portion of the amplitude,

producing the slightly simpler amplitude

$$\begin{aligned}
V_{clas} = & -\frac{8816}{135\pi} \frac{G^2 m^2 m_1 m_2}{r} - \frac{1109}{45\pi} \frac{G^2 m^2 m_1 m_2 e^{-mr}}{r} \\
& + \frac{1}{4\pi} \frac{G^2 e^{-mr}}{r} \left[\left[240m_1 m_2^7 + 530m^2 m_1 m_2^5 + 405m_2^8 + 1620m^2 m_2^6 \right. \right. \\
& \quad - 1085m^6 m_1 m_2 - 240m^6 m_2^2 + 615m^4 m_1 m_2^3 \\
& \quad \left. \left. + 1665m^4 m_2^4 + 2680m^6 m_1 m_2 - 2880m^4 m_1 m_2^3 \right] \log\left(\frac{m_2^2}{m^2}\right) \right. \\
& + \left[405m_1^8 - 240m_1^7 m_2 - 1620m^2 m_1^6 - 530m^2 m_1^5 m_2 + 1085m^6 m_1 m_2 \right. \\
& \quad \left. + 240m^6 m_1^2 - 1665m^4 m_1^4 - 615m^4 m_1^3 m_2 + 2680m^6 m_1 m_2 \right. \\
& \quad \left. \left. - 2880m^4 m_1^3 m_2 \right] \log\left(\frac{m_1^2}{m^2}\right) \right] \quad (8.15)
\end{aligned}$$

This expression for the classical potential has both similarities and differences to the original massless graviton potential. All of the terms have the G^2 and mass dependence characteristic of the second order terms. In addition, most of the terms have an exponential decay term like seen in the tree level potential for the massive graviton. This makes sense, since would expect these terms to take similar form. There are also many mass modification terms which are again similar to those seen in the tree level potential.

However, there are also major differences from the previous results. None of these terms are proportional to $\frac{1}{r^2}$ as we saw in the massless case. Instead, they are all dependent on $\frac{1}{r}$. Now, these are still clearly second order contributions due to their mass and G dependence and their size is suppressed due to factors of the tiny graviton mass, but it is still unexpected to find this r dependence. There are also some new log dependences on the various masses. This is somewhat expected from the form of the integrals, but it does introduce another issue. When we attempt to take the limit as the graviton mass $m \rightarrow 0$, the potential becomes singular. While this is different from what we saw previously, it is not all together unexpected for it to occur in this limit due to the vDVZ discontinuity (see Section 3.3).

8.5 Results for Quantum Diagrams

As we attempted the calculation of the box and crossed box diagrams, two issues arose. Firstly, we were unable to calculate the $C_{\mu\nu\alpha\beta\gamma}$ integral that we needed for this amplitude. The calculation, which boiled down to solving an arbitrary system

of 12 equations for 12 variables, used over 12GB of RAM from the computer that we were using and still did not finish the calculation.

Additionally, we realized that our method of solving these integrals was for integrals in a specific form that held for all of the integrals except for those used in the box and crossed box diagrams. Specifically, the triangle integrals needed to be in the form

$$\int \frac{d^4\ell}{(2\pi)^4} \frac{D(\ell, p_1, \dots, m_1, \dots)}{(\ell^2 - m_1^2)((\ell \pm p_1) - m_2^2)((\ell \pm p_2) - m_3^2)} \quad (8.16)$$

However, since the diagrams have a fourth propagator, and thereby a third momentum p_3 , the FeynCalc function `ScalarProductCancel` put the triangle integrals into a form more like

$$\int \frac{d^4\ell}{(2\pi)^4} \frac{D(\ell, p_1, \dots, m_1, \dots)}{(\ell^2 - m_1^2)((\ell \pm p_1 \pm p_3) - m_2^2)((\ell \pm p_2 \pm p_3) - m_3^2)} \quad (8.17)$$

Thus, in order to continue to use the Passerino-Veltman decomposition, we would need to include all the permutations of including p_3 in the solution for the integral. While not physically impossible, this dramatically increases the number of coefficients needing to be solved for. In fact, in this method, when we tried to solve for $C_{\mu\nu\alpha}$, it required a system of 13 equations with 13 variables. Since we had already not been able to solve the system of 12 equations and variables, we knew that these calculations were simply infeasible given our limited resources. Once we realized this, we knew we would be unable to finish the quantum amplitude calculations. However, even though we were unable to calculate the full modification to the quantum potential due to the difficulties with the box and crossed box diagrams, we were still able to make excellent progress on this calculation. We here list the uncontracted amplitudes for the box and crossed box diagrams as well as the full amplitudes and potentials for all the other quantum diagrams.

The Box and Crossed Box Diagrams

Unfortunately, due to the extra complication of the various integrals needed by these two diagrams, we were unable to find the full contracted and simplified amplitudes.

We here show the uncontracted versions

$$\begin{aligned}
iM_{2a} = & \int \frac{d^4l}{(2\pi)^4} \tau_1^{\mu\nu}(k_1, k_1 + l, m_1) \tau_1^{\rho\sigma}(k_1 + l, k_2, m_1) \tau_1^{\alpha\beta}(k_3, k_3 - l, m_2) \tau_1^{\gamma\delta}(k_3 - l, k_4, m_2) \\
& \times \left[\frac{i}{(k_1 + l)^2 - m_1^2} \right] \left[\frac{i}{(k_3 - l)^2 - m_2^2} \right] \left[\frac{iPm_{\mu\nu\alpha\beta}}{l^2 - m^2} \right] \left[\frac{iPm_{\rho\sigma\gamma\delta}}{(l + q)^2 - m^2} \right]
\end{aligned} \tag{8.18}$$

$$\begin{aligned}
iM_{2b} = & \int \frac{d^4l}{(2\pi)^4} \tau_1^{\mu\nu}(k_1, k_1 + l, m_1) \tau_1^{\rho\sigma}(k_1 + l, k_2, m_1) \tau_1^{\gamma\delta}(k_3, k_4 + l, m_2) \tau_1^{\alpha\beta}(k_4 + l, k_4, m_2) \\
& \times \left[\frac{i}{(k_1 + l)^2 - m_1^2} \right] \left[\frac{i}{(k_3 - l)^2 - m_2^2} \right] \left[\frac{iPm_{\mu\nu\alpha\beta}}{l^2 - m^2} \right] \left[\frac{iPm_{\rho\sigma\gamma\delta}}{(l + q)^2 - m^2} \right]
\end{aligned} \tag{8.19}$$

The Double-Seagull Diagram

Given the change to a massive graviton, the new uncontracted amplitude for the double-seagull diagram (see 6.3) takes the form

$$M_{4a}(q) = \frac{1}{2!} \int \frac{d^4l}{(2\pi)^4} \tau_2^{\alpha\beta\gamma\delta}(k_1, k_2, m_1) \tau_2^{\mu\nu\sigma\rho}(k_3, k_4, m_2) \left[\frac{iPm_{\gamma\delta\sigma\rho}}{l^2 - m^2} \right] \left[\frac{iPm_{\alpha\beta\mu\nu}}{(l + q)^2 - m^2} \right] \tag{8.20}$$

We note the inclusion of the symmetry factor $1/2!$ due to the symmetry of the diagram. We were able to simplify the amplitude via Mathematica and remove all analytic and higher order nonanalytic terms. Under the nonrelativistic approximation, the amplitude takes the form

$$\begin{aligned}
iM_{4a} = & -\frac{32iG^2}{45q^2} \left(271m^2m_1m_2 \log\left(-\frac{m^2}{q^2}\right) - 168m^2m_1m_2 \right) \\
& + \frac{2iG^2}{135m_1m_2} \left(11595m_1^2m_2^2 - 1296m^2m_1^2 - 4926m^2m_1m_2 + 1948m^2m_1m_2 \right. \\
& \left. - 1296m^2m_2^2 \right) \log\left(-\frac{m^2}{q^2}\right)
\end{aligned} \tag{8.21}$$

With a Fourier transform, we derive the contribution to the potential for the double seagull diagram

$$\begin{aligned}
V_{4a} = & \frac{8672G^2m^2m_1m_2}{45} \int \frac{d^3q}{(2\pi)^3} e^{iq \cdot r} \frac{\log(-q^2)}{q^2} - \frac{1344}{45q^2} \frac{G^2m^2m_1m_2}{r} \\
& + \frac{G^2}{135m_1m_2\pi r^3} \left(11595m_1^2m_2^2 - 1296m^2m_1^2 - 4926m^2m_1m_2 \right. \\
& \left. + 1948m^2m_1m_2 - 1296m^2m_2^2 \right)
\end{aligned} \tag{8.22}$$

The Fully Quantum Vertex Correction Diagrams

We next examine the two vertex correction diagrams (see 5.cd in 6.4) which only contribute to the quantum portion of the amplitude and potential. Again, the changes to the uncontracted amplitude are minor and we still include the symmetry factor $1/2!$.

$$M_{5c}(q) = \frac{1}{2!} \int \frac{d^4l}{(2\pi)^4} \tau_2^{\lambda\kappa\phi\epsilon}(k_3, k_4, m_2) \tau_1^{\alpha\beta}(k_1, k_2, m_1) \tau_3^{(\gamma\delta)\mu\nu\rho\sigma}(l, -q) \\ \times \left[\frac{iPm_{\mu\nu\lambda\kappa}}{l^2 - m^2} \right] \left[\frac{iPm_{\sigma\rho\phi\epsilon}}{(l+q)^2 - m^2} \right] \left[\frac{iPm_{\alpha\beta\gamma\delta}}{q^2 - m^2} \right] \quad (8.23)$$

$$M_{5d}(q) = \frac{1}{2!} \int \frac{d^4l}{(2\pi)^4} \tau_2^{\rho\sigma\mu\nu}(k_1, k_2, m_1) \tau_1^{\lambda\kappa}(k_3, k_4, m_2) \tau_3^{(\phi\epsilon)\alpha\beta\gamma\delta}(-l, q) \\ \times \left[\frac{iPm_{\mu\nu\gamma\delta}}{l^2 - m^2} \right] \left[\frac{iPm_{\sigma\rho\alpha\beta}}{(l+q)^2 - m^2} \right] \left[\frac{iPm_{\lambda\kappa\phi\epsilon}}{q^2 - m^2} \right] \quad (8.24)$$

These two diagrams simplify dramatically once run through the Mathematica pipeline. The nonrelativistic, Taylor expanded amplitudes become

$$M_{5c} = \frac{8iG^2}{405 (q^2 - m^2)} \left(4496m^2m_1m_2 \log\left(-\frac{m^2}{q^2}\right) + 2145m^2m_1m_2 \right) \quad (8.25)$$

$$M_{5d} = \frac{8iG^2}{405 (q^2 - m^2)} \left(5922m^2m_1m_2 \log\left(-\frac{m^2}{q^2}\right) + 85m^2m_1m_2 \right) \quad (8.26)$$

We can then Fourier transform the expression to get the quantum contribution to the potential

$$V_{5c} = -\frac{35968G^2m^2m_1m_2}{405} \int \frac{d^3q}{(2\pi)^3} e^{iq\cdot r} \frac{\log(-q^2)}{(q^2 - m^2)} + \frac{286}{27\pi} \frac{G^2m^2m_1m_2e^{-mr}}{r} \quad (8.27)$$

$$V_{5d} = -\frac{47376G^2m^2m_1m_2}{405} \int \frac{d^3q}{(2\pi)^3} e^{iq\cdot r} \frac{\log(-q^2)}{(q^2 - m^2)} + \frac{34}{81\pi} \frac{G^2m^2m_1m_2e^{-mr}}{r} \quad (8.28)$$

Adding the two potentials together, we get

$$V_{5c+5d} = -\frac{83344G^2m^2m_1m_2}{405} \int \frac{d^3q}{(2\pi)^3} e^{iq\cdot r} \frac{\log(-q^2)}{(q^2 - m^2)} + \frac{892}{81\pi} \frac{G^2m^2m_1m_2e^{-mr}}{r} \quad (8.29)$$

The Vacuum Polarization Diagrams

Now for the vacuum polarization diagrams, we are no longer able to use the vacuum polarization tensor as we did for the massless case. Instead, we separately calculate

the two vacuum polarization diagrams with a graviton and ghost loop, respectively (see 6.5). For the ghost loop diagram, we use the massless ghost propagator and the 2ghost-graviton vertex factor gotten from Holstein as seen in Appendix A [21]. The uncontracted amplitudes take the form seen below

$$M_{6a}(q) = \frac{1}{2!} \int \frac{d^4}{(2\pi)^4} \tau_1^{\rho\sigma}(k_1, k_2, m_1) \tau_3^{\lambda\eta\alpha\beta}{}_{\phi\epsilon}(-\ell, -q) \tau_3^{\mu\nu\psi\xi}{}_{i\theta}(l, q) \tau_1^{\gamma\delta}(k_3, k_4, m_2) \\ \times \left[\frac{iPm_{\rho\sigma\lambda\eta}}{q^2 - m^2} \right] \left[\frac{iPm_{\alpha\beta\psi\xi}}{(\ell + q)^2 - m^2} \right] \left[\frac{iPm_{\phi\epsilon i\theta}}{(-\ell)^2 - m^2} \right] \left[\frac{iPm_{\mu\nu\gamma\delta}}{q^2 - m^2} \right] \quad (8.30)$$

$$M_{6b}(q) = \frac{1}{2!} \int \frac{d^4}{(2\pi)^4} \tau_1^{\rho\sigma}(k_1, k_2, m_1) \tau_g^{\lambda\eta\alpha\phi}{}_{\phi\epsilon}(-\ell, -q) \tau_g^{\mu\nu\beta\epsilon}{}_{i\theta}(l, q) \tau_1^{\gamma\delta}(k_3, k_4, m_2) \\ \times \left[\frac{iPm_{\rho\sigma\lambda\eta}}{q^2 - m^2} \right] \left[\frac{i\eta_{\alpha\beta}}{(\ell + q)^2 - m^2} \right] \left[\frac{i\eta_{\phi\epsilon}}{(-\ell)^2 - m^2} \right] \left[\frac{iPm_{\mu\nu\gamma\delta}}{q^2 - m^2} \right] \quad (8.31)$$

After undergoing contraction and simplification, we integrate and Taylor expand. We note that the ghost is massless, so we use the integrals from [5] instead of our newly calculated ones. The simplified version of the amplitudes take the form

$$iM_{6a} = \frac{iG^2}{405 (q^2 - m^2)} \left(54469m^2m_1m_2 \log\left(-\frac{m^2}{q^2}\right) + 4124m^2m_1m_2 \right) \quad (8.32)$$

$$iM_{6b} = -\frac{56iG^2m^2m_1m_2}{45 (q^2 - m^2)} \log(-q^2) \quad (8.33)$$

With a Fourier transform, these expressions become the expected potential terms

$$V_{6a} = -\frac{54469G^2m^2m_1m_2}{405} \int \frac{d^3q}{(2\pi)^3} e^{iq\cdot r} \frac{\log(-q^2)}{(q^2 - m^2)} + \frac{1031}{405\pi} \frac{G^2m^2m_1m_2 e^{-mr}}{r} \quad (8.34)$$

$$V_{6b} = -\frac{56G^2m^2m_1m_2}{45} \int \frac{d^3q}{(2\pi)^3} e^{iq\cdot r} \frac{\log(-q^2)}{(q^2 - m^2)} \quad (8.35)$$

*Chapter 9***FUTURE WORK**

While we have found a satisfying end to this project, there are many more avenues down which it can be taken in the future. While we do not expect the quantum terms to contribute majorly to calculations of black hole inspirals, it is possible that they could be larger than expected. It is thus important to finish running all of the quantum diagrams through our Mathematica pipeline. In order to finish the last two diagrams, the box and cross box, we would need to calculate all the integrals which we could not find before. This would probably require a computer with more processing power and memory than the one we were using. By finishing this calculation, we would thus be able to compare both the classical and quantum terms to those in the massless graviton case and see how their dynamics differ.

Once this calculation is finished, the next step would be to create inspiral models from these potential terms and apply them to LIGO data. By comparing their predictions, it is possible to test the theory of massive gravity against general relativity to see which one fits the physical data better.

One way to confirm our results would be to rederive these amplitudes and thereby potentials via color-kinematic duality between gluons and gravitons. This provides a method to simplify the calculation, while also independently confirm our results. We discussed this option further in Appendix E.

Another possible path forward would be to include extra interactions that would be suggested by the massive graviton theory. Since a massive graviton is predicted in multiple theories beyond the Standard Model, it could be important to add the other particle interactions and see how that might change the resultant potential. It would thereby produce a good means of testing some of these theories in addition to the basic massive gravity theory.

BIBLIOGRAPHY

- [1] Yashar Akrami, S.F. Hassan, Frank Könnig, Angnis Schmidt-May, and Adam R. Solomon. Bimetric gravity is cosmologically viable. *Phys. Lett. B*, 748:37–44, 2015. doi: 10.1016/j.physletb.2015.06.062.
- [2] Zvi Bern, Clifford Cheung, Radu Roiban, Chia-Hsien Shen, Mikhail P. Solon, and Mao Zeng. Black Hole Binary Dynamics from the Double Copy and Effective Theory. *JHEP*, 10:206, 2019. doi: 10.1007/JHEP10(2019)206.
- [3] L. Bernus, O. Minazzoli, A. Fienga, M. Gastineau, J. Laskar, and P. Deram. Constraining the mass of the graviton with the planetary ephemeris INPOP. *Phys. Rev. Lett.*, 123(16):161103, 2019. doi: 10.1103/PhysRevLett.123.161103.
- [4] N. Bjerrum-Bohr, John Donoghue, and B. Holstein. Quantum corrections to the schwarzschild and kerr metrics. *Physical Review D*, 68, 11 2002. doi: 10.1103/PhysRevD.68.084005.
- [5] N. E. J Bjerrum-Bohr, John F. Donoghue, and Barry R. Holstein. Quantum gravitational corrections to the nonrelativistic scattering potential of two masses. *Phys. Rev.*, D67:084033, 2003. doi: 10.1103/PhysRevD.71.069903, 10.1103/PhysRevD.67.084033. [Erratum: *Phys. Rev.* D71,069903(2005)].
- [6] D.G. Boulware and Stanley Deser. Can gravitation have a finite range? *Phys. Rev. D*, 6:3368–3382, 1972. doi: 10.1103/PhysRevD.6.3368.
- [7] Clifford Cheung. TASI Lectures on Scattering Amplitudes. In *Proceedings, Theoretical Advanced Study Institute in Elementary Particle Physics : Anticipating the Next Discoveries in Particle Physics (TASI 2016): Boulder, CO, USA, June 6-July 1, 2016*, pages 571–623, 2018. doi: 10.1142/9789813233348_0008.
- [8] S.R. Choudhury, Girish C. Joshi, S. Mahajan, and Bruce H.J. McKellar. Probing large distance higher dimensional gravity from lensing data. *Astropart. Phys.*, 21:559–563, 2004. doi: 10.1016/j.astropartphys.2004.04.001.
- [9] Diego A.R. Dalvit and Francisco D. Mazzitelli. Running coupling constants, Newtonian potential and nonlocalities in the effective action. *Phys. Rev. D*, 50: 1001–1009, 1994. doi: 10.1103/PhysRevD.50.1001.
- [10] Ganesh Devaraj and Robin G. Stuart. Reduction of one loop tensor form-factors to scalar integrals: A General scheme. *Nucl. Phys.*, B519:483–513, 1998. doi: 10.1016/S0550-3213(98)00035-2.

- [11] John F. Donoghue. Introduction to the effective field theory description of gravity. In *Advanced School on Effective Theories Almunecar, Spain, June 25-July 1, 1995*, 1995.
- [12] John F. Donoghue. The effective field theory treatment of quantum gravity. *AIP Conf. Proc.*, 1483(1):73–94, 2012. doi: 10.1063/1.4756964.
- [13] R.Keith Ellis and Giulia Zanderighi. Scalar one-loop integrals for QCD. *JHEP*, 02:002, 2008. doi: 10.1088/1126-6708/2008/02/002.
- [14] R.Keith Ellis, Zoltan Kunszt, Kirill Melnikov, and Giulia Zanderighi. One-loop calculations in quantum field theory: from Feynman diagrams to unitarity cuts. *Phys. Rept.*, 518:141–250, 2012. doi: 10.1016/j.physrep.2012.01.008.
- [15] Marc H. Goroff and Augusto Sagnotti. The Ultraviolet Behavior of Einstein Gravity. *Nucl. Phys.*, B266:709–736, 1986. doi: 10.1016/0550-3213(86)90193-8.
- [16] David J Griffiths. *Introduction to elementary particles; 2nd rev. version*. Physics textbook. Wiley, New York, NY, 2008. URL <https://cds.cern.ch/record/111880>.
- [17] S.F. Hassan and Rachel A. Rosen. On Non-Linear Actions for Massive Gravity. *JHEP*, 07:009, 2011. doi: 10.1007/JHEP07(2011)009.
- [18] S.F. Hassan and Rachel A. Rosen. Bimetric Gravity from Ghost-free Massive Gravity. *JHEP*, 02:126, 2012. doi: 10.1007/JHEP02(2012)126.
- [19] Kurt Hinterbichler. Theoretical Aspects of Massive Gravity. *Rev. Mod. Phys.*, 84:671–710, 2012. doi: 10.1103/RevModPhys.84.671.
- [20] Barry R. Holstein and Andreas Ross. Spin Effects in Long Range Electromagnetic Scattering. 2008.
- [21] Barry R. Holstein and Andreas Ross. Spin Effects in Long Range Gravitational Scattering. 2008.
- [22] Tristan Hübsch. *Advanced Concepts in Particle and Field Theory*. Cambridge University Press, 2015. doi: 10.1017/CBO9781316160725.
- [23] Y. Iwasaki. Quantum theory of gravitation vs. classical theory. - fourth-order potential. *Prog. Theor. Phys.*, 46:1587–1609, 1971. doi: 10.1143/PTP.46.1587.
- [24] Henrik Johansson and Alexander Ochirov. Color-Kinematics Duality for QCD Amplitudes. *JHEP*, 01:170, 2016. doi: 10.1007/JHEP01(2016)170.
- [25] Henrik Johansson and Alexander Ochirov. Double copy for massive quantum particles with spin. *JHEP*, 09:040, 2019. doi: 10.1007/JHEP09(2019)040.

- [26] I.B. Khriplovich and G.G. Kirilin. Quantum power correction to the Newton law. *J. Exp. Theor. Phys.*, 95(6):981–986, 2002. doi: 10.1134/1.1537290.
- [27] Michele Levi. Binary dynamics from spin1-spin2 coupling at fourth post-Newtonian order. *Phys. Rev. D*, 85:064043, 2012. doi: 10.1103/PhysRevD.85.064043.
- [28] R. Mertig, M. Bohm, and Ansgar Denner. FEYN CALC: Computer algebraic calculation of Feynman amplitudes. *Comput. Phys. Commun.*, 64:345–359, 1991. doi: 10.1016/0010-4655(91)90130-D.
- [29] Ivan J. Muzinich and Stamatis Vokos. Long range forces in quantum gravity. *Phys. Rev. D*, 52:3472–3483, 1995. doi: 10.1103/PhysRevD.52.3472.
- [30] J. C. Romao. *Advanced Quantum Field Theory*. Instituto Superior Tecnico, 2019. URL <http://porthos.tecnico.ulisboa.pt/Public/textos/tca.pdf>.
- [31] Vladyslav Shtabovenko, Rolf Mertig, and Frederik Orellana. New Developments in FeynCalc 9.0. *Comput. Phys. Commun.*, 207:432–444, 2016. doi: 10.1016/j.cpc.2016.06.008.
- [32] Mark Srednicki. *Quantum Field Theory*. Cambridge Univ. Press, Cambridge, 2007. URL <https://cds.cern.ch/record/1019751>.
- [33] K. S. Stelle. Classical Gravity with Higher Derivatives. *Gen. Rel. Grav.*, 9: 353–371, 1978. doi: 10.1007/BF00760427.
- [34] Gerard 't Hooft and M.J.G. Veltman. One loop divergencies in the theory of gravitation. *Ann. Inst. H. Poincare Phys. Theor. A*, 20:69–94, 1974.
- [35] M.J.G. Veltman. Quantum Theory of Gravitation. *Conf. Proc. C*, 7507281: 265–327, 1975.

Appendix A

VERTICES AND PROPAGATORS

Below we list the Feynman rules that were used in our calculation. For a derivation, see [4, 11, 12].

A.1 Massive Scalar Propagator

$$\begin{array}{c} \text{---} \blacktriangleright \text{---} \\ q \end{array} = \frac{i}{q^2 - m^2 + i\epsilon} \quad (\text{A.1})$$

A.2 Massless Graviton Propagator

$$\alpha\beta \begin{array}{c} \text{~~~~~} \\ \text{~~~~~} \\ \text{~~~~~} \\ q \end{array} \gamma\delta = \frac{iP^{\alpha\beta\gamma\delta}}{q^2 + i\epsilon} \quad (\text{A.2})$$

where

$$P^{\alpha\beta\gamma\delta} = \frac{1}{2} [\eta^{\alpha\gamma}\eta^{\beta\delta} + \eta^{\alpha\delta}\eta^{\beta\gamma} - \frac{2}{D-2}\eta^{\alpha\beta}\eta^{\gamma\delta}] \quad (\text{A.3})$$

A.3 Massive Graviton Propagator

$$\alpha\beta \begin{array}{c} \text{~~~~~} \\ \text{~~~~~} \\ \text{~~~~~} \\ q \end{array} \gamma\delta = \frac{iP_m^{\alpha\beta\gamma\delta}(q, m)}{q^2 + i\epsilon} \quad (\text{A.4})$$

where

$$P_m^{\alpha\beta\gamma\delta}(q, m) = \frac{1}{2} \left[F_m^{\alpha\gamma}(q, m)F_m^{\beta\delta}(q, m) + F_m^{\alpha\delta}(q, m)F_m^{\beta\gamma}(q, m) - \frac{2}{D-1}F_m^{\alpha\beta}(q, m)F_m^{\gamma\delta}(q, m) \right] \quad (\text{A.5})$$

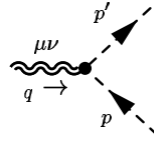
and

$$F_m^{\alpha\beta}(q, m) = \eta^{\alpha\beta} + \frac{q^\alpha q^\beta}{m^2} \quad (\text{A.6})$$

A.4 Massless Ghost Propagator

$$\begin{array}{c} b \text{ ---} \blacktriangleleft \text{ ---} a \\ p \end{array} = \frac{i\eta^{\alpha\beta}}{p^2 + i\epsilon} \quad (\text{A.7})$$

A.5 2 Scalar, 1 Graviton Vertex Factor

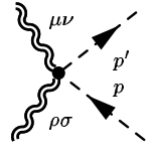


$$= \tau_1^{\mu\nu}(p, p', m)$$

where

$$\tau_1^{\mu\nu}(p, p', m) = -\frac{i\kappa}{2} [p^\mu p'^\nu + p'^\mu p^\nu - \eta^{\mu\nu}((p \cdot p') - m^2)] \quad (\text{A.8})$$

A.6 2 Scalar, 2 Graviton Vertex Factor



$$= \tau_2^{\mu\nu\rho\sigma}(p, p', m)$$

where

$$\begin{aligned} \tau_2^{\mu\nu\rho\sigma}(p, p', m) = i\kappa^2 & \left[\left(I^{\mu\nu\alpha\delta} I^{\rho\sigma\beta\delta} - \frac{1}{4} [\eta^{\mu\nu} I^{\rho\sigma\alpha\beta} + \eta^{\rho\sigma} I^{\mu\nu\alpha\beta}] \right) (p_\alpha p'_\beta + p'_\alpha p_\beta) \right. \\ & \left. - \frac{1}{2} \left(I^{\mu\nu\rho\sigma} - \frac{1}{2} \eta^{\mu\nu} \eta^{\rho\sigma} \right) [(p \cdot p') - m^2] \right] \quad (\text{A.9}) \end{aligned}$$

and

$$I^{\alpha\beta\gamma\delta} = \frac{1}{2} (\eta^{\alpha\gamma} \eta^{\beta\delta} + \eta^{\alpha\delta} \eta^{\beta\gamma}) \quad (\text{A.10})$$

A.7 3 Graviton Vertex Factor

$$= \tau_{3\alpha\beta\gamma\delta}^{\mu\nu}(k, q)$$

where

$$\begin{aligned} \tau_{3\alpha\beta\gamma\delta}^{\mu\nu}(k, q) = & -\frac{i\kappa}{2} \left(P^{\alpha\beta\gamma\delta} \left[k^\mu k^\nu + (k+q)^\mu (k+q)^\nu + q^\mu q^\nu - \frac{3}{2} \eta^{\mu\nu} q^2 \right] \right. \\ & + 2q_\lambda q_\sigma \left[I_{\alpha\beta}^{\sigma\lambda} I_{\gamma\delta}^{\mu\nu} + I_{\gamma\delta}^{\sigma\lambda} I_{\alpha\beta}^{\mu\nu} - I_{\alpha\beta}^{\mu\sigma} I_{\gamma\delta}^{\nu\lambda} - I_{\gamma\delta}^{\mu\sigma} I_{\alpha\beta}^{\nu\lambda} \right] \\ & + \left[q_\lambda q^\mu \left(\eta_{\alpha\beta} I_{\gamma\delta}^{\nu\lambda} + \eta_{\gamma\delta} I_{\alpha\beta}^{\nu\lambda} \right) + q_\lambda q^\nu \left(\eta_{\alpha\beta} I_{\gamma\delta}^{\mu\lambda} + \eta_{\gamma\delta} I_{\alpha\beta}^{\mu\lambda} \right) \right. \\ & \left. - q^2 \left(\eta_{\alpha\beta} I_{\gamma\delta}^{\mu\nu} + \eta_{\gamma\delta} I_{\alpha\beta}^{\mu\nu} \right) - \eta^{\mu\nu} q_\lambda q^\sigma \left(\eta_{\alpha\beta} I_{\gamma\delta}^{\sigma\lambda} + \eta_{\gamma\delta} I_{\alpha\beta}^{\sigma\lambda} \right) \right] \\ & + \left[2q_\lambda \left(I_{\alpha\beta}^{\lambda\sigma} I_{\gamma\delta\sigma}{}^\nu (k-q)^\mu + I_{\alpha\beta}^{\lambda\sigma} I_{\gamma\delta\sigma}{}^\mu (k-q)^\nu - I_{\gamma\delta}^{\lambda\sigma} I_{\alpha\beta\sigma}{}^\nu k^\mu - I_{\gamma\delta}^{\lambda\sigma} I_{\alpha\beta\sigma}{}^\mu k^\nu \right) \right. \\ & \left. + q^2 \left(I_{\alpha\beta\sigma}{}^\mu I_{\gamma\delta}{}^{\nu\sigma} + I_{\gamma\delta\sigma}{}^\mu I_{\alpha\beta}{}^{\nu\sigma} \right) + \eta^{\mu\nu} q_\sigma q_\lambda \left(I_{\alpha\beta}^{\lambda\rho} I_{\gamma\delta\rho}{}^\sigma + I_{\gamma\delta}^{\lambda\rho} I_{\alpha\beta\rho}{}^\sigma \right) \right] \\ & \left. + \left[(k^2 + (k-q)^2) \left[I_{\alpha\beta}^{\mu\sigma} I_{\gamma\delta\sigma}{}^\nu + I_{\gamma\delta}^{\mu\sigma} I_{\alpha\beta\sigma}{}^\nu - \frac{1}{2} \eta^{\mu\nu} P_{\alpha\beta\gamma\delta} \right] - \left(I_{\gamma\delta}^{\mu\nu} \eta_{\alpha\beta} k^2 + I_{\alpha\beta}^{\mu\nu} \eta_{\gamma\delta} (k-q)^2 \right) \right] \right] \end{aligned} \quad (\text{A.11})$$

A.8 2 Ghost, 1 Graviton Vertex Factor

$$= \tau_g^{\mu\nu}{}_{\alpha\beta}(k, q)$$

where

$$\begin{aligned} \tau_g^{\mu\nu}{}_{\alpha\beta}(k, q) = & \frac{i\kappa}{2} \left[(k^2 + (k+q)^2 + q^2) I_{\alpha\beta}^{\mu\nu} + 2\eta_{\alpha\beta} k^\lambda (k+q)^\sigma P_{\lambda\sigma}{}^{\mu\nu} \right. \\ & \left. + 2q_\alpha k^\lambda I_{\beta\lambda}^{\mu\nu} - 2q_\beta (k+q)^\lambda I_{\alpha\lambda}^{\mu\nu} + q_\alpha q_\beta \eta^{\mu\nu} \right] \end{aligned} \quad (\text{A.12})$$

Appendix B

INTEGRALS USED IN THE MASSLESS CASE

We recreate the integrals used in the massless case here due to some copy errors noted in the integrals given by [5].

B.1 Bubble Integrals

$$I = \int \frac{d^4\ell}{(2\pi)^4} \frac{1}{\ell^2(\ell+q)^2} = \frac{i}{16\pi^2} [-L] + \dots \quad (\text{B.1})$$

$$I_\mu = \int \frac{d^4\ell}{(2\pi)^4} \frac{\ell_\mu}{\ell^2(\ell+q)^2} = \frac{i}{16\pi^2} \left[\frac{1}{2} q_\mu L \right] + \dots \quad (\text{B.2})$$

$$I_{\mu\nu} = \int \frac{d^4\ell}{(2\pi)^4} \frac{\ell_\mu \ell_\nu}{\ell^2(\ell+q)^2} = \frac{i}{16\pi^2} \left[\frac{1}{12} L q^2 \eta_{\mu\nu} - \frac{1}{3} L q_\mu q_\nu \right] + \dots \quad (\text{B.3})$$

$$I_{\mu\nu\alpha} = \int \frac{d^4\ell}{(2\pi)^4} \frac{\ell_\mu \ell_\nu \ell_\alpha}{\ell^2(\ell+q)^2} = \frac{i}{16\pi^2} \left[-\frac{1}{24} L q^2 3\eta_{(\mu\nu} q_{\alpha)} + \frac{1}{4} L q_\mu q_\nu q_\alpha \right] + \dots \quad (\text{B.4})$$

$$I_{\mu\nu\alpha\beta} = \int \frac{d^4\ell}{(2\pi)^4} \frac{\ell_\mu \ell_\nu \ell_\alpha \ell_\beta}{\ell^2(\ell+q)^2} = \frac{i}{16\pi^2} \left[-\frac{1}{240} L q^4 3\eta_{(\mu\nu} \eta_{\alpha\beta)} \right. \\ \left. + \frac{1}{40} L q^2 6\eta_{(\mu\nu} q_\alpha q_\beta) - \frac{1}{5} L q_\mu q_\nu q_\alpha q_\beta + \dots \right] \quad (\text{B.5})$$

where $L = \log(-q^2)$ and $S = \frac{\pi^2}{\sqrt{-q^2}}$, and analytic and higher order nonanalytic terms are represented by the ellipses.

B.2 Triangle Integrals

$$J = \int \frac{d^4\ell}{(2\pi)^4} \frac{1}{\ell^2(\ell+q)^2((\ell+k)^2 - m_1^2)} \\ = \frac{i}{32\pi^2 m_1^2} [-L - S] + \dots \quad (\text{B.6})$$

$$J_\mu = \int \frac{d^4\ell}{(2\pi)^4} \frac{\ell_\mu}{\ell^2(\ell+q)^2((\ell+k)^2 - m_1^2)} \\ = \frac{i}{32\pi^2 m_1^2} \left[k_\mu \left(\left(-1 - \frac{1}{2} \frac{q^2}{m_1^2} \right) L - \frac{1}{4} \frac{q^2}{m_1^2} S \right) + q_\mu q_\nu \left(L + \frac{1}{2} S \right) \right] + \dots \quad (\text{B.7})$$

$$\begin{aligned}
J_{\mu\nu} &= \int \frac{d^4\ell}{(2\pi)^4} \frac{\ell_\mu \ell_\nu}{\ell^2(\ell+q)^2((\ell+k)^2-m_1^2)} \\
&= \frac{i}{32\pi^2 m_1^2} \left[k_\mu k_\nu \left(-\frac{1}{2} \frac{q^2}{m_1^2} L - \frac{1}{8} \frac{q^2}{m_1^2} S \right) + q_\mu \left(-L - \frac{3}{8} S \right) \right. \\
&\quad \left. + 2q_{(\mu} k_{\nu)} \left(\left(\frac{1}{2} + \frac{1}{2} \frac{q^2}{m_1^2} \right) L + \frac{3}{16} \frac{q^2}{m_1^2} S \right) + q^2 \eta_{\mu\nu} \left(\frac{1}{4} L + \frac{1}{8} S \right) \right] + \dots \tag{B.8}
\end{aligned}$$

$$\begin{aligned}
J_{\mu\nu\alpha} &= \int \frac{d^4\ell}{(2\pi)^4} \frac{\ell_\mu \ell_\nu \ell_\alpha}{\ell^2(\ell+q)^2((\ell+k)^2-m_1^2)} \\
&= \frac{i}{32\pi^2 m_1^2} \left[k_\mu k_\nu k_\alpha \left(-\frac{1}{6} \frac{q^2}{m_1^2} L \right) + q_\mu q_\nu q_\alpha \left(L + \frac{5}{16} S \right) \right. \\
&\quad + 3q_{(\mu} k_{\nu} k_{\alpha)} \left(\frac{1}{3} \frac{q^2}{m_1^2} L + \frac{1}{16} \frac{q^2}{m_1^2} S \right) + 3q_{(\mu} q_{\nu} k_{\alpha)} \left(\left(-\frac{1}{3} - \frac{1}{2} \frac{q^2}{m_1^2} \right) L - \frac{5}{32} \frac{q^2}{m_1^2} S \right) \\
&\quad \left. + 3\eta_{(\mu\nu} k_{\alpha)} \left(q^2 \frac{1}{12} q^2 L \right) + 3\eta_{(\mu\nu} q_{\alpha)} \left(-\frac{1}{6} q^2 L - \frac{1}{16} q^2 S \right) \right] + \dots \tag{B.9}
\end{aligned}$$

where $L = \log(-q^2)$ and $S = \frac{\pi^2}{\sqrt{-q^2}}$, and analytic and higher order non-analytic terms are represented by the ellipses. We utilize the symmetrization convention used by [20] where

$$A_{(\mu_1\mu_2\mu_3\dots\mu_n)} = \frac{1}{n!} (A_{\mu_1\mu_2\mu_3\dots\mu_n} + A_{(\mu_2\mu_1\mu_3\dots\mu_n)} + \dots) \tag{B.10}$$

For example, this means that $3\eta_{(\mu\nu} q_{\alpha)} = \eta_{\mu\nu} q_\alpha + \eta_{\mu\alpha} q_\nu + \eta_{\alpha\nu} q_\mu$.

B.3 Box and Cross Box Integrals

$$\begin{aligned}
K &= \int \frac{d^4\ell}{(2\pi)^4} \frac{1}{\ell^2(\ell+q)^2((\ell+k_1)^2-m_1^2)((\ell-k_3)^2-m_2^2)} \\
&= \frac{i}{16\pi^2 m_1 m_2} \left[\frac{L}{q^2} \left(1 - \frac{s-s_0}{6m_1 m_2} \right) - i2\pi \frac{L}{q^2} \frac{1}{2\sqrt{m_1 m_2} \sqrt{s-s_0}} \left(1 - \frac{s-s_0}{8m_1 m_2} \right) \right] \tag{B.11}
\end{aligned}$$

$$\begin{aligned}
K' &= \int \frac{d^4\ell}{(2\pi)^4} \frac{1}{\ell^2(\ell+q)^2((\ell+k_1)^2-m_1^2)((\ell+k_4)^2-m_2^2)} \\
&= \frac{i}{16\pi^2 m_1 m_2} \left[-\frac{L}{q^2} \left(1 - \frac{s-s_0}{6m_1 m_2} \right) \right] \tag{B.12}
\end{aligned}$$

Appendix C

INTEGRALS USED IN THE MASSIVE CASE

C.1 Tadpole and Bubble Integrals

$$A_0(m) = \int \frac{d^4\ell}{(2\pi)^4} \frac{1}{(\ell^2 - m^2)} = 0 \quad (\text{C.1})$$

$$\begin{aligned} B_0 &= \int \frac{d^4\ell}{(2\pi)^4} \frac{1}{(\ell^2 - m_1^2)((\ell + q)^2 - m_2^2)} \\ &= \frac{i}{16\pi^2} \frac{1}{q^2} \left(-\frac{m_1^2 - m_2^2}{2} \log\left(\frac{m_1^2}{m_2^2}\right) + SL(q, m_1, m_2) \right) \end{aligned} \quad (\text{C.2})$$

$$\begin{aligned} B_\mu &= \int \frac{d^4\ell}{(2\pi)^4} \frac{\ell_\mu}{(\ell^2 - m_1^2)((\ell + q)^2 - m_2^2)} \\ &= \frac{i}{32\pi^2} q_\mu \left(-\frac{1}{q^2} - \frac{1}{q^4} (m_1^2 - m_2^2) \right) SL(q, m_1, m_2) \\ &\quad + \frac{i}{64\pi^2 q^4} q_\mu \left((m_1^2 - m_2^2)^2 \right) \log\left(\frac{m_1^2}{m_2^2}\right) \end{aligned} \quad (\text{C.3})$$

$$\begin{aligned} B_{\mu\nu} &= \int \frac{d^4\ell}{(2\pi)^4} \frac{\ell_\mu \ell_\nu}{(\ell^2 - m_1^2)((\ell + q)^2 - m_2^2)} \\ &= \frac{i}{16\pi^2} \left[\left(\frac{m_1^2 + m_2^2}{6} \frac{1}{q^2} - \frac{1}{12} \right) \eta_{\mu\nu} + \left(\frac{m_1^2 - 2m_2^2}{3} \frac{1}{q^4} + \frac{1}{3} \frac{1}{q^2} \right) q_\mu q_\nu \right] SL(q, m_1, m_2) \\ &\quad + \frac{i}{16\pi^2} (m_1^2 - m_2^2)^3 \left[\left(\frac{1}{24} \frac{1}{q^4} \right) \eta_{\mu\nu} + \left(-\frac{1}{6} \frac{1}{q^6} \right) q_\mu q_\nu \right] \log\left(\frac{m_1^2}{m_2^2}\right) \\ &\quad + \frac{i}{16\pi^2} (m_1^2 - m_2^2)^2 \left[\left(-\frac{1}{12} \frac{1}{q^4} \right) \eta_{\mu\nu} + \left(\frac{1}{3} \frac{1}{q^6} \right) q_\mu q_\nu \right] SL(q, m_1, m_2) \end{aligned} \quad (\text{C.4})$$

$$\begin{aligned} B_{\mu\nu\alpha} &= \int \frac{d^4\ell}{(2\pi)^4} \frac{\ell_\mu \ell_\nu \ell_\alpha}{(\ell^2 - m_1^2)((\ell + q)^2 - m_2^2)} \\ &= \frac{i}{16\pi^2} \left[\left(-\frac{m_1^2 + 3m_2^2}{24} \frac{1}{q^2} + \frac{1}{24} \right) 3\eta_{(\mu\nu} q_{\alpha)} - \left(\frac{m_1^2 - 3m_2^2}{4} \frac{1}{q^4} \right. \right. \\ &\quad \left. \left. + \frac{1}{4} \frac{1}{q^2} \right) q_\mu q_\nu q_\alpha \right] SL(q, m_1, m_2) \\ &\quad + \frac{i}{16\pi^2} (m_1^2 - m_2^2)^4 \left[\left(-\frac{1}{48} \frac{1}{q^6} \right) 3\eta_{(\mu\nu} q_{\alpha)} + \left(\frac{1}{8} \frac{1}{q^8} \right) q_\mu q_\nu q_\alpha \right] \log\left(\frac{m_1^2}{m_2^2}\right) \end{aligned}$$

$$\begin{aligned}
& + \frac{i}{16\pi^2} (m_1^2 - m_2^2)^3 \left[\left(\frac{1}{24} \frac{1}{q^6} \right) \eta_{(\mu\nu} q_\alpha) + \left(-\frac{1}{4} \frac{1}{q^8} \right) q_\mu q_\nu q_\alpha \right] SL(q, m_1, m_2) \\
& + \frac{i}{16\pi^2} (m_1^2 - m_2^2) \left[\left(-\frac{m_1^2 + 3m_2^2}{24} \frac{1}{q^4} \right) \eta_{(\mu\nu} q_\alpha) \right. \\
& \quad \left. + \left(-\frac{m_1^2 - 3m_2^2}{4} \frac{1}{q^6} \right) q_\mu q_\nu q_\alpha \right] SL(q, m_1, m_2)
\end{aligned} \tag{C.5}$$

$$\begin{aligned}
B_{\mu\nu\alpha\beta} &= \int \frac{d^4\ell}{(2\pi)^4} \frac{\ell_\mu \ell_\nu \ell_\alpha \ell_\beta}{(\ell^2 - m_1^2)((\ell + q)^2 - m_2^2)} = \\
&= \frac{i}{16\pi^2} \left[\left(\frac{3m_1^4 + 2m_1^2 m_2^2 + 3m_2^4}{120} \frac{1}{q^2} - \frac{m_1^2 + m_2^2}{60} + \frac{q^2}{240} \right) 6\eta_{(\mu\nu} \eta_{\alpha\beta)} \right. \\
& \quad + \left(\frac{m_1^4 + 4m_1^2 m_2^2 - 9m_2^4}{60} \frac{1}{q^4} + \frac{m_1^2 + 6m_2^2}{60} - \frac{1}{40} \right) 6\eta_{(\mu\nu} q_\alpha q_\beta) \\
& \quad \left. + \left(\frac{m_1^4 - 6m_1^2 m_2^2 + 6m_2^4}{5} \frac{1}{q^6} + \frac{m_1^2 - 4m_2^2}{5} \frac{1}{q^2} + \frac{1}{5} \frac{1}{q^2} \right) q_\mu q_\nu q_\alpha q_\beta \right] SL(q, m_1, m_2) \\
& + \frac{i}{16\pi^2} (m_1^2 - m_2^2)^5 \left[\left(-\frac{1}{480} \frac{1}{q^6} \right) 6\eta_{(\mu\nu} \eta_{\alpha\beta)} + \left(\frac{1}{80} \frac{1}{q^8} \right) 6\eta_{(\mu\nu} q_\alpha q_\beta) + \right. \\
& \quad \left. \left(-\frac{1}{10} \frac{1}{q^{10}} \right) q_\mu q_\nu q_\alpha q_\beta \right] \log \left(\frac{m_1^2}{m_2^2} \right) \\
& + \frac{i}{16\pi^2} (m_1^2 - m_2^2)^4 \left[\left(\frac{1}{240} \frac{1}{q^6} \right) 6\eta_{(\mu\nu} \eta_{\alpha\beta)} + \left(-\frac{1}{40} \frac{1}{q^8} \right) 6\eta_{(\mu\nu} q_\alpha q_\beta) \right. \\
& \quad \left. + \left(\frac{1}{5} \frac{1}{q^{10}} \right) q_\mu q_\nu q_\alpha q_\beta \right] SL(q, m_1, m_2) \\
& + \frac{i}{16\pi^2} (m_1^2 - m_2^2)^2 \left[\left(-\frac{m_1^2 + m_2^2}{60} \frac{1}{q^4} \right) 6\eta_{(\mu\nu} \eta_{\alpha\beta)} + \left(\frac{m_1^2 + 6m_2^2}{60} \frac{1}{q^6} \right) 6\eta_{(\mu\nu} q_\alpha q_\beta) \right. \\
& \quad \left. + \left(\frac{m_1^2 - 4m_2^2}{5} \frac{1}{q^8} \right) q_\mu q_\nu q_\alpha q_\beta \right] SL(q, m_1, m_2)
\end{aligned} \tag{C.6}$$

$$\begin{aligned}
B_{\mu\nu\alpha\beta\gamma} &= \int \frac{d^4\ell}{(2\pi)^4} \frac{\ell_\mu \ell_\nu \ell_\alpha \ell_\beta \ell_\gamma}{(\ell^2 - m_1^2)((\ell + q)^2 - m_2^2)} \\
&= \frac{i}{16\pi^2} \left[\left(-\frac{m_1^4 + 2m_1^2 m_2^2 + 5m_2^4}{240} \frac{1}{q^2} + \frac{3m_1^2 + 5m_2^2}{480} - \frac{q^2}{480} \right) 15\eta_{(\mu\nu} \eta_{\alpha\beta} q_\gamma) \right. \\
& \quad + \left(-\frac{m_1^4 + 7m_1^2 m_2^2 - 20m_2^4}{120} \frac{1}{q^4} - \frac{m_1^2 + 10m_2^4}{120} + \frac{1}{60} \right) 10\eta_{(\mu\nu} q_\alpha q_\beta q_\gamma) \\
& \quad \left. + \left(-\frac{m_1^4 - 8m_1^2 m_2^2 + 10m_2^4}{6} \frac{1}{q^6} - \frac{m_1^2 - 5m_2^2}{6} \frac{1}{q^4} - \frac{1}{6} \frac{1}{q^2} \right) q_\mu q_\nu q_\alpha q_\beta \right] SL(q, m_1, m_2)
\end{aligned}$$

$$\begin{aligned}
& + \frac{i}{16\pi^2} (m_1^2 - m_2^2)^6 \left[\left(\frac{1}{960} \frac{1}{q^8} \right) 15\eta(\mu\nu\eta_{\alpha\beta}q_\gamma) + \left(-\frac{1}{120} \frac{1}{q^{10}} \right) 10\eta(\mu\nu q_\alpha q_\beta q_\gamma) \right. \\
& \quad \left. + \left(\frac{1}{12} \frac{1}{q^{12}} \right) q_\mu q_\nu q_\alpha q_\beta q_\gamma \right] \log\left(\frac{m_1^2}{m_2^2}\right) \\
& + \frac{i}{16\pi^2} (m_1^2 - m_2^2)^5 \left[\left(-\frac{1}{480} \frac{1}{q^8} \right) 15\eta(\mu\nu\eta_{\alpha\beta}q_\gamma) + \left(\frac{1}{60} \frac{1}{q^8} \right) 10\eta(\mu\nu q_\alpha q_\beta q_\gamma) \right. \\
& \quad \left. + \left(-\frac{1}{6} \frac{1}{q^{12}} \right) q_\mu q_\nu q_\alpha q_\beta q_\gamma \right] SL(q, m_1, m_2) \\
& + \frac{i}{16\pi^2} (m_1^2 - m_2^2)^3 \left[\left(\frac{3m_1^2 + 5m_2^2}{480} \frac{1}{q^6} \right) 15\eta(\mu\nu\eta_{\alpha\beta}q_\gamma) \right. \\
& \quad + \left(-\frac{m_1^2 + 10m_2^2}{120} \frac{1}{q^8} \right) 10\eta(\mu\nu q_\alpha q_\beta q_\gamma) \\
& \quad \left. + \left(-\frac{m_1^2 - 5m_2^2}{6} \frac{1}{q^{10}} \right) q_\mu q_\nu q_\alpha q_\beta q_\gamma \right] SL(q, m_1, m_2) \\
& - \frac{i}{16\pi^2} (m_1^2 - m_2^2) \left[\left(\frac{m_1^4 + 2m_1^2 m_2^2 + 5m_2^4}{240} \frac{1}{q^4} \right) 15\eta(\mu\nu\eta_{\alpha\beta}q_\gamma) \right. \\
& \quad + \left(\frac{m_1^4 + 7m_1^2 m_2^2 - 20m_2^4}{120} \frac{1}{q^6} \right) 10\eta(\mu\nu q_\alpha q_\beta q_\gamma) \\
& \quad \left. + \left(\frac{m_1^4 - 8m_1^2 m_2^2 + 10m_2^4}{6} \frac{1}{q^8} \right) q_\mu q_\nu q_\alpha q_\beta q_\gamma \right] SL(q, m_1, m_2) \tag{C.7}
\end{aligned}$$

$$\begin{aligned}
B_{\mu\nu\alpha\beta\gamma\delta} &= \int \frac{d^4\ell}{(2\pi)^4} \frac{\ell_\mu \ell_\nu \ell_\alpha \ell_\beta \ell_\gamma \ell_\delta}{(\ell^2 - m_1^2)((\ell + q)^2 - m_2^2)} \\
&= \frac{i}{16\pi^2} \left[\left(\frac{(m_1^2 + m_2^2)(5m_1^4 - 2m_1^2 m_2^2 + 5m_2^4)}{1680} \frac{1}{q^2} - \frac{5m_1^4 + 6m_1^2 m_2^2 + 5m_2^4}{2240} \right. \right. \\
& \quad \left. \left. + q^2 \frac{m_1^2 + m_2^2}{1120} - \frac{q^4}{6720} \right) 15\eta(\mu\nu\eta_{\alpha\beta}\eta_{\gamma\delta}) \right. \\
& + \left(\frac{m_1^6 + 2m_1^4 m_2^2 + 9m_1^2 m_2^4 - 20m_2^6}{210} \frac{1}{q^4} - \frac{m_1^4 + 4m_1^2 m_2^2 + 15m_2^4}{840} \frac{1}{q^2} \right. \\
& \quad \left. - \frac{5m_1^2 + 12m_2^2}{1680} - \frac{q^2}{840} \right) 45\eta(\mu\nu\eta_{\alpha\beta}q_\gamma q_\delta) \\
& + \left(\frac{m_1^6 + 9m_1^4 m_2^2 - 54m_1^2 m_2^4 + 50m_2^6}{210} \frac{1}{q^6} + \frac{2m_1^4 + 22m_1^2 m_2^2 - 75m_2^4}{420} \frac{1}{q^4} \right. \\
& \quad \left. + \frac{m_1^2 + 15m_2^2}{210} - \frac{1}{84} \right) 15\eta(\mu\nu\eta_{\alpha\beta}q_\gamma q_\delta) \\
& + \left(\frac{(m_1^2 - 2m_2^2)(m_1^4 - 10m_1^2 m_2^2 + 10m_2^4)}{7} \frac{1}{q^8} + \frac{(m_1^4 - 10m_1^2 m_2^2 + 15m_2^4)}{7} \frac{1}{q^6} \right.
\end{aligned}$$

$$\begin{aligned}
& + \left. \frac{m_1^2 - 6m_2^2}{7} \frac{1}{q^4} + \frac{1}{7} \frac{1}{q^2} \right) q_\mu q_\nu q_\alpha q_\beta q_\gamma q_\delta \Big] SL(q, m_1, m_2) \\
& + \frac{i}{16\pi^2} (m_1^2 - m_2^2)^7 \left[\left(\frac{1}{13440} \frac{1}{q^8} \right) 15\eta(\mu\nu\eta_\alpha\beta\eta_\gamma\delta) + \left(-\frac{1}{1680} \frac{1}{q^{10}} \right) 45\eta(\mu\nu\eta_\alpha\beta q_\gamma q_\delta) \right. \\
& \quad \left. + \left(\frac{1}{168} \frac{1}{q^{12}} \right) 15\eta(\mu\nu q_\alpha q_\beta q_\gamma q_\delta) + \left(-\frac{1}{14} \frac{1}{q^{14}} \right) q_\mu q_\nu q_\alpha q_\beta q_\gamma q_\delta \right] \log\left(\frac{m_1^2}{m_2^2}\right) \\
& + \frac{i}{16\pi^2} (m_1^2 - m_2^2)^6 \left[\left(-\frac{1}{6720} \frac{1}{q^8} \right) 15\eta(\mu\nu\eta_\alpha\beta\eta_\gamma\delta) + \left(\frac{1}{840} \frac{1}{q^{10}} \right) 45\eta(\mu\nu\eta_\alpha\beta q_\gamma q_\delta) \right. \\
& \quad \left. + \left(-\frac{1}{84} \frac{1}{q^{12}} \right) 15\eta(\mu\nu q_\alpha q_\beta q_\gamma q_\delta) + \left(\frac{1}{7} \frac{1}{q^{14}} \right) q_\mu q_\nu q_\alpha q_\beta q_\gamma q_\delta \right] SL(q, m_1, m_2) \\
& + \frac{i}{16\pi^2} (m_1^2 - m_2^2)^4 \left[\left(\frac{m_1^2 + m_2^2}{1120} \frac{1}{q^6} \right) 15\eta(\mu\nu\eta_\alpha\beta\eta_\gamma\delta) \right. \\
& \quad \left. + \left(-\frac{5m_1^2 + 12m_2^2}{1680} \frac{1}{q^8} \right) 45\eta(\mu\nu\eta_\alpha\beta q_\gamma q_\delta) + \left(\frac{m_1^2 + 15m_2^2}{210} \frac{1}{q^{10}} \right) 15\eta(\mu\nu q_\alpha q_\beta q_\gamma q_\delta) \right. \\
& \quad \left. + \left(\frac{m_1^2 - 6m_2^2}{7} \frac{1}{q^{12}} \right) q_\mu q_\nu q_\alpha q_\beta q_\gamma q_\delta \right] SL(q, m_1, m_2) \\
& - \frac{i}{16\pi^2} (m_1^2 - m_2^2)^2 \left[\left(\frac{5m_1^4 + 6m_1^2 m_2^2 + 5m_2^4}{2240} \frac{1}{q^4} \right) 15\eta(\mu\nu\eta_\alpha\beta\eta_\gamma\delta) \right. \\
& \quad + \left(\frac{m_1^4 + 4m_1^2 m_2^2 + 15m_2^4}{840} \frac{1}{q^6} \right) 45\eta(\mu\nu\eta_\alpha\beta q_\gamma q_\delta) \\
& \quad + \left(\frac{2m_1^4 + 22m_1^2 m_2^2 - 75m_2^4}{420} \frac{1}{q^8} \right) 15\eta(\mu\nu q_\alpha q_\beta q_\gamma q_\delta) \\
& \quad \left. + \left(\frac{m_1^4 - 10m_1^2 m_2^2 + 15m_2^4}{7} \frac{1}{q^{10}} \right) q_\mu q_\nu q_\alpha q_\beta q_\gamma q_\delta \right] SL(q, m_1, m_2) \quad (C.8)
\end{aligned}$$

C.2 Triangle Integrals

We used the C_0 integral as defined by [10]

$$\begin{aligned}
C_0 &= \int \frac{d^4\ell}{(2\pi)^4} \frac{1}{(\ell^2 - m_1^2)((\ell + k_1)^2 - m_2^2)((\ell + k_2)^2 - m_3^2)} \\
&= \frac{k_1^2 B_0(k_1, m_1, m_2) + ((k_1 \cdot k_2) - k_1^2) B_0(k_1 + k_2, m_1, m_3) - (k_1 \cdot k_2) B_0(k_1, m_2, m_3)}{-(k_1 \cdot k_2) f_1 - k_1^2 f_2} \quad (C.9)
\end{aligned}$$

where

$$f_1 = m_1^2 - m_2^2 - k_1^2 \quad (C.10)$$

$$f_2 = m_2^2 - m_3^2 + k_1^2 - (k_1 - k_2)^2 \quad (C.11)$$

All other non-scalar triangle integrals used were decomposed in terms of the C_0 , B_0 , and A_0 integrals. Each integral has the inputs $C(q, k_1, m, m, m_1)$. We have Taylor expanded the expressions with respect to the graviton mass m up to order 2 and the exchanged momentum q up to order 4. We also only record the nonanalytic terms of these expressions.

$$\begin{aligned}
C_\mu &= \int \frac{d^4\ell}{(2\pi)^4} \frac{\ell_\mu}{(\ell^2 - m_1^2)((\ell + k_1)^2 - m_2^2)((\ell + k_2)^2 - m_3^2)} \\
&= -\frac{i}{64\pi^2 m_1^2 q^2} m^2 \left(8k_1^\mu \log\left(-\frac{m^2}{q^2}\right) - q^\mu \log\left(\frac{m^2}{m_1^2}\right) - 2q^\mu \log\left(-\frac{m^2}{q^2}\right) \right) \\
&\quad - \frac{i}{128\pi^2 m_1^4} \left(-8m_1^2 k_1^\mu \log\left(-\frac{m^2}{q^2}\right) + 6m^2 k_1^\mu \log\left(-\frac{m^2}{q^2}\right) + 4m_1^2 q^\mu \log\left(-\frac{m^2}{q^2}\right) \right) \\
&\quad - 2m^2 q^\mu \log\left(-\frac{m^2}{q^2}\right) + \frac{i}{1024\pi^2 m_1^6} q^2 \left(16m_1^2 k_1^\mu \log\left(-\frac{m^2}{q^2}\right) - 16m^2 k_1^\mu \log\left(-\frac{m^2}{q^2}\right) \right) \\
&\quad - 8m_1^2 q^\mu \log\left(-\frac{m^2}{q^2}\right) + 6m^2 q^\mu \log\left(-\frac{m^2}{q^2}\right) - \frac{i}{2048\pi^2 m_1^8} q^4 \left(-8m_1^2 k_1^\mu \log\left(-\frac{m^2}{q^2}\right) \right) \\
&\quad + 10m^2 k_1^\mu \log\left(-\frac{m^2}{q^2}\right) + 4m_1^2 q^\mu \log\left(-\frac{m^2}{q^2}\right) - 4m^2 q^\mu \log\left(-\frac{m^2}{q^2}\right) + O\left(m^3, q^5\right)
\end{aligned}$$

$$\begin{aligned}
C_{\mu\nu} &= \int \frac{d^4\ell}{(2\pi)^4} \frac{\ell_\mu \ell_\nu}{(\ell^2 - m_1^2)((\ell + k_1)^2 - m_2^2)((\ell + k_2)^2 - m_3^2)} \\
&= -\frac{i}{128\pi^2 m_1^2 q^2} \left(-8m^2 k_1^\nu q^\mu \log\left(-\frac{m^2}{q^2}\right) - 8m^2 k_1^\mu q^\nu \log\left(-\frac{m^2}{q^2}\right) - m^2 q^\mu q^\nu \log\left(\frac{m^2}{m_1^2}\right) + 6m_1^2 q^\mu q^\nu \log\left(\frac{m^2}{m_1^2}\right) \right) \\
&\quad + \frac{i}{256\pi^2 m_1^4} \left(16m^2 m_1^2 \log\left(-\frac{m^2}{q^2}\right) g^{\mu\nu} - 8m_1^2 k_1^\nu q^\mu \log\left(-\frac{m^2}{q^2}\right) \right) \\
&\quad - 8m_1^2 k_1^\mu q^\nu \log\left(-\frac{m^2}{q^2}\right) - 40m^2 k_1^\mu k_1^\nu \log\left(-\frac{m^2}{q^2}\right) + 24m^2 k_1^\nu q^\mu \log\left(-\frac{m^2}{q^2}\right) \\
&\quad + 24m^2 k_1^\mu q^\nu \log\left(-\frac{m^2}{q^2}\right) + 10m_1^2 q^\mu q^\nu \log\left(-\frac{m^2}{q^2}\right) - 18m^2 q^\mu q^\nu \log\left(-\frac{m^2}{q^2}\right) \\
&\quad - \frac{i}{2048\pi^2 m_1^6} q^2 \left(16m_1^4 \log\left(-\frac{m^2}{q^2}\right) g^{\mu\nu} - 32m^2 m_1^2 \log\left(-\frac{m^2}{q^2}\right) g^{\mu\nu} \right) \\
&\quad - 48m_1^2 k_1^\mu k_1^\nu \log\left(-\frac{m^2}{q^2}\right) + 40m_1^2 k_1^\nu q^\mu \log\left(-\frac{m^2}{q^2}\right) + 40m_1^2 k_1^\mu q^\nu \log\left(-\frac{m^2}{q^2}\right) \\
&\quad + 160m^2 k_1^\mu k_1^\nu \log\left(-\frac{m^2}{q^2}\right) - 88m^2 k_1^\nu q^\mu \log\left(-\frac{m^2}{q^2}\right) - 88m^2 k_1^\mu q^\nu \log\left(-\frac{m^2}{q^2}\right)
\end{aligned}$$

$$-32m_1^2 q^\mu q^\nu \log\left(-\frac{m^2}{q^2}\right) + 56m^2 q^\mu q^\nu \log\left(-\frac{m^2}{q^2}\right) + O\left(m^3, q^3\right)$$

$$\begin{aligned} C_{\mu\nu\alpha} &= \int \frac{d^4\ell}{(2\pi)^4} \frac{\ell_\mu \ell_\nu \ell_\alpha}{(\ell^2 - m_1^2)((\ell + k_1)^2 - m_2^2)((\ell + k_2)^2 - m_3^2)} \\ &= \frac{11im^2 q^\alpha q^\mu q^\nu \log\left(\frac{m^2}{m_1^2}\right)}{128\pi^2 q^4} - \frac{i}{256\pi^2 m_1^2 q^2} \left(6m^2 m_1^2 q^\alpha \log\left(\frac{m^2}{m_1^2}\right) g^{\mu\nu} \right. \\ &\quad + 6m^2 m_1^2 q^\mu \log\left(\frac{m^2}{m_1^2}\right) g^{\alpha\nu} + 6m^2 m_1^2 q^\nu \log\left(\frac{m^2}{m_1^2}\right) g^{\alpha\mu} - 6m^2 k_1^\alpha k_1^\nu q^\alpha \log\left(\frac{m^2}{m_1^2}\right) \\ &\quad - 6m^2 k_1^\alpha k_1^\mu q^\mu \log\left(\frac{m^2}{m_1^2}\right) - 19m^2 k_1^\nu q^\alpha q^\mu \log\left(\frac{m^2}{m_1^2}\right) - 6m^2 k_1^\alpha k_1^\mu q^\nu \log\left(\frac{m^2}{m_1^2}\right) \\ &\quad - 19m^2 k_1^\mu q^\alpha q^\nu \log\left(\frac{m^2}{m_1^2}\right) - 19m^2 k_1^\alpha q^\mu q^\nu \log\left(\frac{m^2}{m_1^2}\right) + 5m_1^2 k_1^\nu q^\alpha q^\mu \log\left(\frac{m^2}{m_1^2}\right) \\ &\quad + 5m_1^2 k_1^\mu q^\alpha q^\nu \log\left(\frac{m^2}{m_1^2}\right) + 5m_1^2 k_1^\alpha q^\mu q^\nu \log\left(\frac{m^2}{m_1^2}\right) - 8m^2 k_1^\nu q^\alpha q^\mu \log\left(-\frac{m^2}{q^2}\right) \\ &\quad - 8m^2 k_1^\mu q^\alpha q^\nu \log\left(-\frac{m^2}{q^2}\right) - 8m^2 k_1^\alpha q^\mu q^\nu \log\left(-\frac{m^2}{q^2}\right) + 51m^2 q^\alpha q^\mu q^\nu \log\left(\frac{m^2}{m_1^2}\right) \\ &\quad + 14m_1^2 q^\alpha q^\mu q^\nu \log\left(\frac{m^2}{m_1^2}\right) + 18m^2 q^\alpha q^\mu q^\nu \log\left(-\frac{m^2}{q^2}\right) \\ &\quad + \frac{i}{6144m_1^4 \pi^2} \left(48m^2 \log\left(-\frac{m^2}{q^2}\right) q^\alpha g^{\mu\nu} m_1^2 + 48m^2 \log\left(-\frac{m^2}{q^2}\right) g^{\alpha\nu} q^\mu m_1^2 \right. \\ &\quad - 16 \log\left(-\frac{m^2}{q^2}\right) q^\alpha q^\mu k_1^\nu m_1^2 + 48m^2 \log\left(-\frac{m^2}{q^2}\right) g^{\alpha\mu} q^\nu m_1^2 \\ &\quad - 16 \log\left(-\frac{m^2}{q^2}\right) q^\alpha k_1^\mu q^\nu m_1^2 - 16 \log\left(-\frac{m^2}{q^2}\right) k_1^\alpha q^\mu q^\nu m_1^2 \\ &\quad + 96 \log\left(-\frac{m^2}{q^2}\right) q^\alpha q^\mu q^\nu m_1^2 + 192m^2 \log\left(-\frac{m^2}{q^2}\right) k_1^\alpha k_1^\mu k_1^\nu \\ &\quad - 240m^2 \log\left(-\frac{m^2}{q^2}\right) q^\alpha k_1^\mu k_1^\nu - 240m^2 \log\left(-\frac{m^2}{q^2}\right) k_1^\alpha q^\mu k_1^\nu \\ &\quad + 264m^2 \log\left(-\frac{m^2}{q^2}\right) q^\alpha q^\mu k_1^\nu - 240m^2 \log\left(-\frac{m^2}{q^2}\right) k_1^\alpha k_1^\mu q^\nu \\ &\quad \left. + 264m^2 \log\left(-\frac{m^2}{q^2}\right) q^\alpha k_1^\mu q^\nu + 264m^2 \log\left(-\frac{m^2}{q^2}\right) k_1^\alpha q^\mu q^\nu \right) \end{aligned}$$

$$\begin{aligned}
& - 276m^2 \log\left(-\frac{m^2}{q^2}\right) q^\alpha q^\mu q^\nu - \frac{i}{12288m_1^6 \pi^2} \left(-32 \log\left(-\frac{m^2}{q^2}\right) k_1^\alpha g^{\mu\nu} m_1^4\right. \\
& + 64 \log\left(-\frac{m^2}{q^2}\right) q^\alpha g^{\mu\nu} m_1^4 - 32 \log\left(-\frac{m^2}{q^2}\right) g^{\alpha\nu} k_1^\mu m_1^4 \\
& + 64 \log\left(-\frac{m^2}{q^2}\right) g^{\alpha\nu} q^\mu m_1^4 - 32 \log\left(-\frac{m^2}{q^2}\right) g^{\alpha\mu} k_1^\nu m_1^4 \\
& + 64 \log\left(-\frac{m^2}{q^2}\right) g^{\alpha\mu} q^\nu m_1^4 + 48m^2 \log\left(-\frac{m^2}{q^2}\right) k_1^\alpha g^{\mu\nu} m_1^2 \\
& - 48m^2 \log\left(-\frac{m^2}{q^2}\right) q^\alpha g^{\mu\nu} m_1^2 + 48m^2 \log\left(-\frac{m^2}{q^2}\right) g^{\alpha\nu} k_1^\mu m_1^2 \\
& - 48m^2 \log\left(-\frac{m^2}{q^2}\right) g^{\alpha\nu} q^\mu m_1^2 + 48m^2 \log\left(-\frac{m^2}{q^2}\right) g^{\alpha\mu} k_1^\nu m_1^2 \\
& + 160 \log\left(-\frac{m^2}{q^2}\right) k_1^\alpha k_1^\mu k_1^\nu m_1^2 - 224 \log\left(-\frac{m^2}{q^2}\right) q^\alpha k_1^\mu k_1^\nu m_1^2 \\
& - 224 \log\left(-\frac{m^2}{q^2}\right) k_1^\alpha q^\mu k_1^\nu m_1^2 + 240 \log\left(-\frac{m^2}{q^2}\right) q^\alpha q^\mu k_1^\nu m_1^2 \\
& - 48m^2 \log\left(-\frac{m^2}{q^2}\right) g^{\alpha\mu} q^\nu m_1^2 - 224 \log\left(-\frac{m^2}{q^2}\right) k_1^\alpha k_1^\mu q^\nu m_1^2 \\
& + 240 \log\left(-\frac{m^2}{q^2}\right) q^\alpha k_1^\mu q^\nu m_1^2 + 240 \log\left(-\frac{m^2}{q^2}\right) k_1^\alpha q^\mu q^\nu m_1^2 \\
& - 248 \log\left(-\frac{m^2}{q^2}\right) q^\alpha q^\mu q^\nu m_1^2 - 432m^2 \log\left(-\frac{m^2}{q^2}\right) k_1^\alpha k_1^\mu k_1^\nu \\
& + 360m^2 \log\left(-\frac{m^2}{q^2}\right) q^\alpha k_1^\mu k_1^\nu + 360m^2 \log\left(-\frac{m^2}{q^2}\right) k_1^\alpha q^\mu k_1^\nu \\
& - 300m^2 \log\left(-\frac{m^2}{q^2}\right) q^\alpha q^\mu k_1^\nu + 360m^2 \log\left(-\frac{m^2}{q^2}\right) k_1^\alpha k_1^\mu q^\nu \\
& - 300m^2 \log\left(-\frac{m^2}{q^2}\right) q^\alpha k_1^\mu q^\nu - 300m^2 \log\left(-\frac{m^2}{q^2}\right) k_1^\alpha q^\mu q^\nu \\
& + 252m^2 \log\left(-\frac{m^2}{q^2}\right) q^\alpha q^\mu q^\nu q^2 + O\left(m^3, q^3\right)
\end{aligned} \tag{C.14}$$

C.3 Box and Cross Box Integrals

We used the D_0 integral as defined by [10]

$$\begin{aligned}
D_0 &= \int \frac{d^4l}{(2\pi)^4} \frac{1}{(l^2 - m_1^2)((l + k_1)^2 - m_2^2)((l + k_2)^2 - m_3^2)((l - k_3)^2 - m_4^2)} \\
&= \frac{1}{Y_3} \left[-x_{33} C_0(k_1, k_2, m_2^2, m_1^2, m_3^2) + (x_{33} - x_{32}) C_0(k_1, -k_3, m_2^2, m_1^2, m_4^2) \right. \\
&\quad \left. + (x_{32} - x_{31}) C_0(k_1 - k_2, k_2 + k_3, m_2^2, m_3^2, m_4^2) + x_{31} C_0(k_2, k_2 + k_3, m_1^2, m_3^2, m_4^2) \right] \quad (\text{C.15})
\end{aligned}$$

$$\begin{aligned}
D'_0 &= \int \frac{d^4l}{(2\pi)^4} \frac{1}{(l^2 - m_1^2)((l + k_1)^2 - m_2^2)((l + k_2)^2 - m_3^2)((l + k_4)^2 - m_4^2)} \\
&= \frac{1}{Y'_3} \left[-x'_{33} C_0(k_1, k_2, m_2^2, m_1^2, m_3^2) + (x'_{33} - x'_{32}) C_0(k_1, k_4, m_2^2, m_1^2, m_4^2) \right. \\
&\quad \left. + (x'_{32} - x'_{31}) C_0(k_1 - k_2, k_2 - k_4, m_2^2, m_3^2, m_4^2) + x'_{31} C_0(k_2, k_2 - k_4, m_1^2, m_3^2, m_4^2) \right] \quad (\text{C.16})
\end{aligned}$$

where

$$f_1 = f'_1 = m_1^2 - m_2^2 - k_1^2 \quad (\text{C.17})$$

$$f_2 = f'_2 = m_2^2 - m_3^2 + k_1^2 - (k_1 - k_2)^2 \quad (\text{C.18})$$

$$f_3 = m_3^2 - m_4^2 + (k_1 - k_2)^2 - (k_1 - k_3)^2 \quad (\text{C.19})$$

$$x_{31} = -(k_1 \cdot k_2)(k_2 \cdot k_3) - (k_1 \cdot k_3)k_2^2 \quad (\text{C.20})$$

$$x_{32} = -(k_1 \cdot k_2)(k_1 \cdot k_3) - (k_2 \cdot k_3)k_1^2 \quad (\text{C.21})$$

$$x_{33} = x'_{33} = k_2^2 k_1^2 - (k_1 \cdot k_2)^2 \quad (\text{C.22})$$

$$Y_3 = x_{31} f_1 + x_{32} f_2 + x_{33} f_3 \quad (\text{C.23})$$

$$f'_3 = m_3^2 - m_4^2 + (k_1 - k_2)^2 - (k_1 + k_4)^2 \quad (\text{C.24})$$

$$x'_{31} = (k_1 \cdot k_2)(k_2 \cdot k_4) + (k_1 \cdot k_4)k_2^2 \quad (\text{C.25})$$

$$x'_{32} = (k_1 \cdot k_2)(k_1 \cdot k_4) + (k_2 \cdot k_4)k_1^2 \quad (\text{C.26})$$

$$Y'_3 = x'_{31} f'_1 + x'_{32} f'_2 + x'_{33} f'_3 \quad (\text{C.27})$$

$$(\text{C.28})$$

All other non-scalar triangle integrals used were decomposed in terms of the D_0 , C_0 , B_0 , and A_0 integrals

Appendix D

FOURIER TRANSFORMS

In this thesis, we make use of many 3D fourier transforms. We have accumulated these from several resources. The three that we use for the massless graviton calculations are listed below [5]:

$$\int \frac{d^3 q}{(2\pi)^3} e^{i\mathbf{q}\cdot\mathbf{r}} \frac{1}{|\mathbf{q}|^2} = \frac{1}{4\pi r} \quad (\text{D.1})$$

$$\int \frac{d^3 q}{(2\pi)^3} e^{i\mathbf{q}\cdot\mathbf{r}} \frac{1}{|\mathbf{q}|} = \frac{1}{2\pi^2 r^2} \quad (\text{D.2})$$

$$\int \frac{d^3 q}{(2\pi)^3} e^{i\mathbf{q}\cdot\mathbf{r}} \ln(\mathbf{q}^2) = -\frac{1}{2\pi r^3} \quad (\text{D.3})$$

$$\int \frac{d^3 q}{(2\pi)^3} e^{i\mathbf{q}\cdot\mathbf{r}} = \delta^3(r) \quad (\text{D.4})$$

$$\int \frac{d^3 q}{(2\pi)^3} e^{i\mathbf{q}\cdot\mathbf{r}} q^2 = \delta^{3''}(r) \quad (\text{D.5})$$

For the massive graviton calculations, we reference [27] and use their transforms as shown below

$$I = \int \frac{d^d q}{(2\pi)^d} e^{i\mathbf{q}\cdot\mathbf{r}} \frac{1}{(\mathbf{q}^2)^\alpha} = \frac{1}{(4\pi)^{d/2}} \frac{\Gamma(d/2 - \alpha)}{\Gamma(\alpha)} \left(\frac{r^2}{4}\right)^{\alpha-d/2} \quad (\text{D.6})$$

$$\int \frac{d^3 q}{(2\pi)^3} e^{i\mathbf{q}\cdot\mathbf{r}} \frac{\log(-q^2)}{q^2} = \quad (\text{D.7})$$

$$\int \frac{d^3 q}{(2\pi)^3} e^{i\mathbf{q}\cdot\mathbf{r}} \frac{\log(-q^2)}{(q^2 - m^2)} = \quad (\text{D.8})$$

Appendix E

COLOR-KINEMATICS DUALITY

At one point in this thesis, we were considering exploring the usefulness of utilizing color-kinematic duality as a way to check our answers. This duality interchanges the color and kinematic structures of the S-matrix. In practice, this means that the amplitudes of various particle interactions can be "squared" to produce an equivalent amplitude for interactions in other theories [24]. We were specifically interested in one such relation, that of "graviton = gluon²" [7]. This means that if we took the expres-

sion for the scattering amplitude for fig. E.1 before integration and squared it, we would get the desired amplitude for the diagram in fig. E.2 Since great progress has already been made with the strong force, we originally thought we could rederive the amplitudes for our project through this independent method. We hoped that enough research would had been done in the field of massive gluons that this could be reasonably simple method to check our conclusions through an independent process. However, after searching into the work done with massive gluons, we realized that while this procedure should work [25], it would require more calculation and effort than expected, since we would have had to calculate the majority of the massive gluon amplitudes that we needed. We expect that this process could be the source of an entirely new project or thesis and suggest this as a possibility to any interested readers.

Figure E.1: A tree level gluon interaction

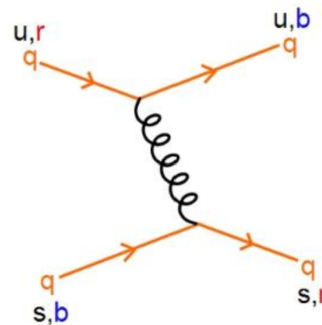


Figure E.2: A tree level graviton interaction

